WAVES GENERATED BY ROCK FALLS INTO RESERVOIRS

Presented as a thesis for the degree

of Master of Engineering

The University of Canterbury

by

M.W.M. Cornwall, B.E. (Hons.)

March, 1971

BKS 532.59 WAV
Waves generated by rock falls into reservoirs [thesis] / M.W.M. Cornwall. - Christchurch : UNiversity of Canterbur
ID: 3008889
BARCODE: 064555

Industrial Research Limited
064555

SYNOPSIS

Since the Vaiont Dam disaster in 1963, there has been an awareness among design engineers of the rockfall problem, where a large landslide into shallow water can generate water waves of appreciable size. The prediction of landslide properties, like size and speed, is qualitative. However, for a given landslide into shallow water, this study aims to provide a quantitative prediction of some important wave properties.

Rectangular blocks were dropped vertically into a long horizontal channel of constant width. The leading or first waves generated were mostly unbroken and, although assymmetrical, were similar to solitary waves. Only large, heavy blocks dropped from well above the water surface caused broken waves, these converting into solitary waves at substantial distances downstream. A long oscillatory wave train followed the leading wave, but because its height was usually smaller and subsided at a greater rate than the leading wave, it was not considered to be important.

The first wave height is related to the block dimensions and density and its fall height. Subsidence is also studied.

ACKNOWLEDGMENTS

Acknowledgments are gratefully made to:

Professor H.J. Hopkins, Head of the Civil Engineering Department, under whose overall guidance this study was made.

Mr. R.F. Hince, Senior Lecturer and supervisor, for his interest, guidance, and assistance.

All other members of the staff who assisted in this study, especially the technical staff whose assistance in developing the experimental equipment is greatly appreciated.

My wife, Barbara, for her understanding and encouragement.

The Ministry of Works and the University Grants Committee for financial aid.

TABLE OF CONTENTS

LIST OF SYMBOLS

a	height of first wave above still water level.
a'	depth of first trough below still water level.
d	height of block.
d'	height above channel floor to which the block falls.
g	acceleration due to gravity.
H	distance through which the block falls.
h_f	depth of water in channel.
l	length of block.
m	exponent relating $\frac{a}{h_f}$ to $\frac{x}{h_f}$ (Ch. 7, Section C).
n	exponent relating $\frac{a}{h_f}$ to $\frac{H+d'}{h_f}$ (Ch. 7, Section A)
u	horizontal component of water velocity underneath the block.
U	horizontal component of velocity of water escaping from under the front face of a falling block.
v	i) vertical component of water velocity underneath the block; ii) velocity of leading crest along channel.
v'	velocity of first trough along channel
V	velocity of falling block just after it strikes the water surface.
V_o	velocity of falling block just before it strikes the water surface.
x	horizontal distance measured from front face of block.
y	distance between channel floor and falling block.
δ	distance between rear of block and end of channel.
λ	distance between first wave crest and first trough.
ρ_f	density of water in channel.
ρ_s	density of block.

CHAPTER 1

INTRODUCTION

There have been several instances recorded where landslides into shallow water have caused large surface waves, often with disastrous consequences. In the case of reservoir dams which are generally designed with small freeboards, even comparatively small waves can cause overtopping. This is not likely to do much structural damage to masonry and concrete dams. However, any overtopping of an earth dam is serious, because the dam material can be washed away with comparative ease. Once the freeboard has been eroded there is every chance that water flowing over the crest will cause complete failure of the dam.

Little is known of the properties of waves generated by landslides into reservoirs. The fact that the size and speed of a landslide can be estimated only roughly compounds the problem.

The aim of this study was to elucidate upon the nature of waves caused by vertical rock falls, for example where a cliff collapses into a reservoir. The experimental part of the study involved modelling the situation by dropping rectangular-sectioned blocks vertically into water at one end of a long, horizontal channel (see Fig. 1.1).

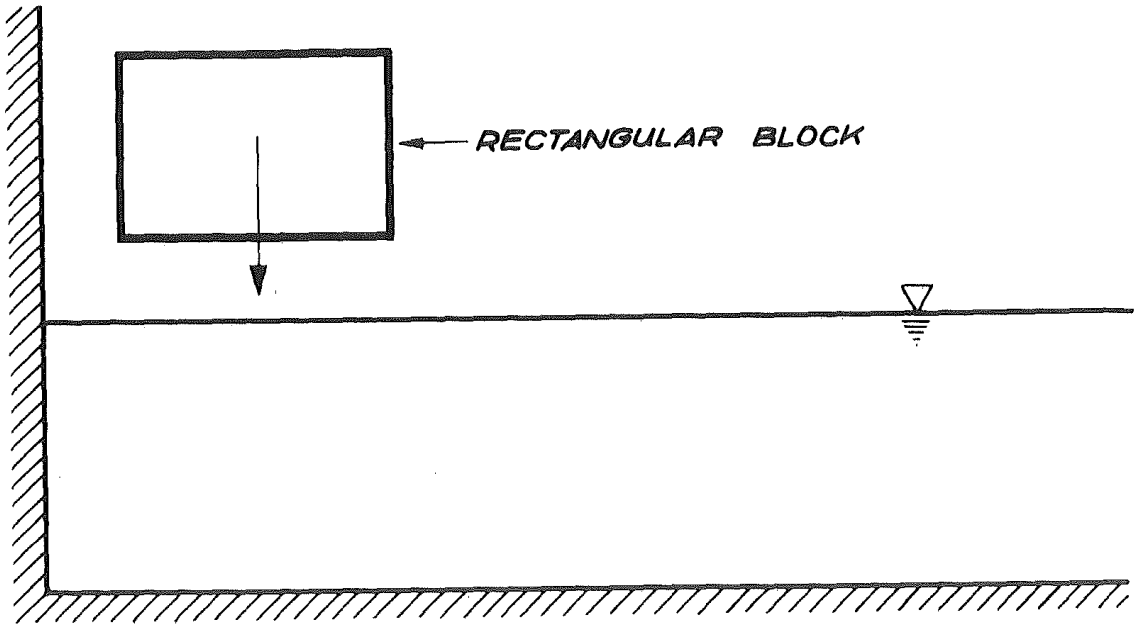

Fig. 1.1

Simple Schematic diagram of experimental study.

Such a simple model is of value but has definite limitations. It can be used to simulate a cliff falling into the end of an arm of a reservoir, or possibly a landslide into a lake in a steep narrow gorge. But a full understanding of the nature of waves generated in this manner will facilitate the study of waves caused by similar volume intrusions, and hopefully will be useful in the search for a comprehensive solution for non-vertical intrusions by volumes of arbitrary shape.

The experimental study showed that vertical intrusions caused two types of waves to proceed down the channel:

(a) a shallow water wave, where movement of water over the whole depth occurs at a speed dependent on the water depth; followed by

(b) an extended deep water oscillatory wave train where movement of water occurs only near the surface. The wave speed is slower than for a shallow water wave and is dependent on wave length.

The shallow water wave tended to be an asymmetrical solitary wave. In cases of large intrusions with high energy, a small surge formed. The deep water wave train was slower moving, dispersive, and generally of smaller amplitude.

A computer simulation was attempted, using a finite difference approach based on a Lagrangian coordinate system; a system which generalises comparatively simply to allow for varying channel depth and, as a later refinement, for varying width. Unfortunately, time did not allow the computer simulation to be developed to the stage where realistic results could be obtained. A finite element approach using Lagrangian coordinates was later formulated for computer use but was not fully developed, preference being given to the experimental studies outlined above.

CHAPTER 2

LITERATURE REVIEW

Previous Research

To date few papers have been published on experimental investigations of the rock-fall problem. Researchers who have studied topics related to the rock-fall problem include:

(a) J.E. Prins [1],

(b) Law and Brebner [2],

(c) R.L. Weigel and associates [3], [4].

A resumé of their lines of study is given below.

J.E. Prins, 1958.

Prins published papers in 1958 on his experimental studies of waves generated by localised initial surface elevations and depressions. These local conditions were created by varying air pressure over an area of water surface at one end of a long channel. A slight vacuum in an enclosure would cause water to rise within it, causing a small elevation. Similarly, a small excess pressure would cause a depression of water surface. Sudden removal of the end of the enclosure allowed the vertical wall of water at the boundary to collapse. The waves created were measured at various points along the channel.

Prins found that for small elevations or depressions and small lengths of enclosure relative to water depth the waves formed were similar to those predicted theoretically by Unoki and Nakano in 1953. These researchers developed an equation for the surface history of a wave generated by the subsidence of a uniform surface elevation of finite length on infinitely deep water. Their equation was:

$$y_s = \frac{4h}{t} \left(\frac{x}{\pi g}\right)^{\frac{1}{2}} \sin \left(\frac{gt^2}{4x} \cdot \frac{\lambda}{x}\right) \cos \left(\frac{gt^2}{4x} - \frac{\pi}{4}\right)$$

where y_s = surface elevation at distance x and time t,

x = distance along channel measured from front of enclosure,

t = time measured from removal of enclosure end,

h = initial surface elevation in enclosure,

λ = length of enclosure,

g = acceleration due to gravity.

This equation gave accurate predictions of wave and wave group properties, but predicted larger amplitude waves than were measured.

For large lengths or heights of enclosures relative to water depth the equation did not hold. Initial surface elevations caused solitary waves followed by small amplitude wave trains. For very large enclosure sizes, broken bores were formed which eventually subsided into a train of complex solitary waves or undular bores. In cases of large initial

depressions of the water surface, a negative wave followed by a dispersive wave train always formed.

Prins derived the following graph (Fig. 2.1) from his results. It relates the wave forms generated to the dimensions of the water in the enclosure.

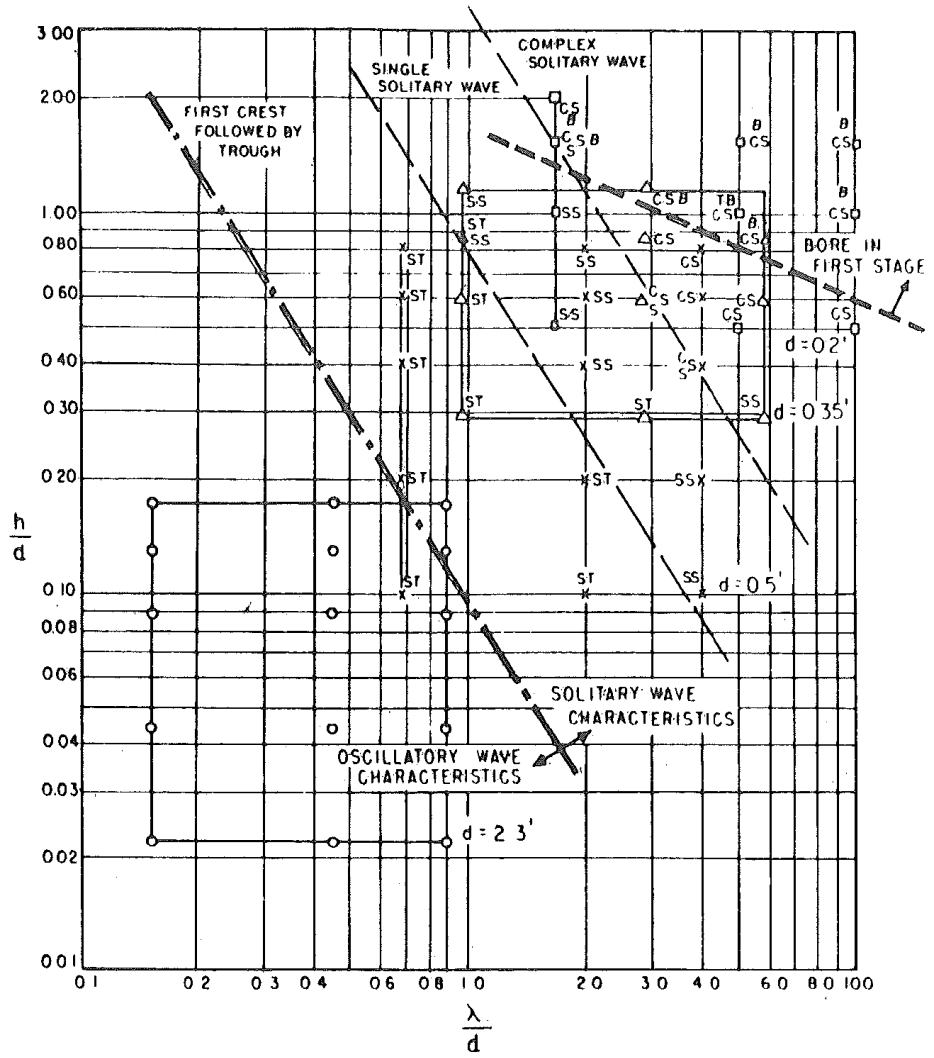

Fig. 2.1. Relationship between $\frac{\lambda}{d}$, $\frac{h}{d}$ and the characteristics of the leading wave for initial elevations where d = water depth (Prins).

Law and Brebner, 1968

Law and Brebner studied waves created by blocks sliding down an inclined slope into a water channel. Their work is marred by a rather inadequate dimensional analysis. Several relationships they derived were dependent on a parameter K where

$$K = \frac{\rho_s}{\rho_w} \cdot \frac{V_i^2}{gd} \cdot \frac{V}{d^3}$$

In the above,

ρ_s = block density,

ρ_w = water density,

V_i = velocity of impact of block as it penetrates the water surface

g = acceleration due to gravity,

V = volume per unit width

d = water depth.

The parameter is not dimensionless. The term V is a measure of a cross-sectional area, i.e. of $(\text{length})^2$; thus the term $\frac{V}{d^3}$ has a dimension of $(\text{length})^{-1}$. The dimensions of the block are allowed for by provision of a parameter involving block height, i.e. since the block area is determined by $\frac{V}{d^3}$ and the height is also determined, it follows that the block length is known, too.

The inclusion of a term $\frac{V_i^2}{gd}$ in the paramter K is a mistake. Chapter 7 describes how wave heights are related

to block densities and dimensions in a different manner to velocities of impact. Inclusion of $\frac{V_i^2}{gd}$ in K without also keeping it as an independent parameter is in contravention of Buckingham's π theorem [5].

As could be expected, there was a large amount of scatter in graphs relating other parameters to K. Although their results show some trends between various parameters, Law and Brebner's paper is of little value in obtaining quantitative predictions of wave heights.

R.L. Weigel

Weigel has published two papers on the study of waves caused by falling blocks. Resumés of these are given below.

(a) Laboratory studies of gravity waves generated by the movement of a submerged body [3], 1955.

The movement of a submarine landslide was simulated by letting a submerged block fall to a channel floor. Two sets of experiments were completed, one with triangular blocks sliding down an inclined board, and another with rectangular blocks either falling vertically or sliding down an incline.

These movements generally caused a small crest followed by a large trough and large second crest to proceed along the channel. Behind these waves a small dispersive wavetrain followed.

The wave heights and periods for the first two crests and first trough were related to

a) water depth,

b) initial depth of submergence of block,

c) submerged weight of block,

d) angle of inclined board.

The usefulness of results is lessened by the absence of dimensional analysis. Results are thus presented in dimensional form, which limits their usefulness.

A comparison between results from much of Weigel's paper and this study is not feasible. The experimental set-up was different in that all blocks were initially fully submerged before they fell. The blocks fell from their submerged position to the channel floor, whereas in this study the blocks fell from above the water surface to some position above the channel floor. Thus quite different areas of water were being displaced by the falling blocks. Also, for a large part of Weigel's study, only two measuring stations were used, one 1.09 ft. and the other 4.82 ft. from the block. Water depths varied between 1.50 ft. and 1.92 ft. Thus these stations measured wave heights in the region of their generation. Measuring stations in this study were placed at points distant from the region of generation.

Some of Weigel's experiments were carried out with four measuring stations spread along a channel, these being at

points 1.09, 11.0, 23.6, and 36.5 ft. from the centre line of the falling block. For these experiments the block was a lead plate of full channel width, 6 in. long, and 3/16th in. deep. The water depth was set at 0.36 ft., 0.24 ft., or 0.14 ft. These runs were compared with results from this study in Chapter 7, "Discussion of Results", section C, below.

(b) Water waves generated by landslides in reservoirs [4], 1970.

The second paper Professor Weigel wrote in conjunction with Messrs. Noda, Kuba, Gee, and Tornberg. It contains a substantial literary review of the works of Prins [1], and several other researchers who confined their interests mainly to theoretical investigations of phenomena related to the rock-fall problem. Prins' work is described above.

Also included in the paper is a large section describing experimental investigations by the Authors. A rockfall was simulated by dropping rectangular boxes into a channel in a manner very similar to the method used in this study.

The main difference in the experimental set-up was that for most of their work blocks were dropped from positions where part of the block was initially submerged.

The analysis of results is not very satisfactory. The variables they considered important are depicted in Fig. 2.2.

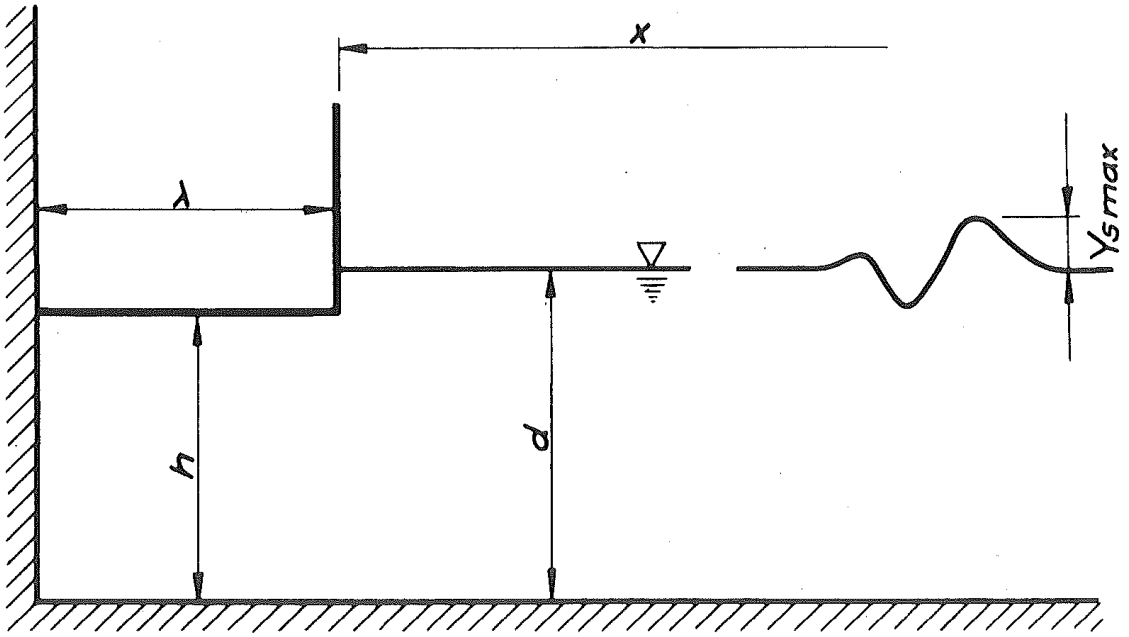

Fig. 2.2 Schematic diagram of experimental set-up (Weigel et al)

namely:

λ = length of block,

h = height of bottom of block above channel floor,

d = water depth,

x = distance along channel measured from front of block,

y_{smax} = height of crest of leading wave above still water level.

Also included were the weight of the box W, and a term

$$\frac{V_{avg}}{(gd)^{\frac{1}{2}}}$$

where V_{avg} = average velocity of box as it fell through the water.

g = acceleration due to gravity.

The parameter $\frac{V_{avg}}{(gd)^{\frac{1}{2}}}$ is not well chosen. It was varied by changing the weight and the fall height of the block. This study shows that both of these block properties are important parameters by themselves. No attempt seems to have been made to relate $\frac{V_{avg}}{(gd)^{\frac{1}{2}}}$ to either the block weight or its fall height, and there is no way of accurately predicting its value. It is not related to any of the measurable quantities found, for instance, at a potential rockfall site.

First wave heights are measured in terms of a parameter $\frac{y_{smax}}{h}$ rather than the more common $\frac{y_{smax}}{d}$. The former parameter may be of use when the water depth, d, is not varied and provided the fall height, h, is either always less than d, when the water under the block is accelerated smoothly as the block starts its fall, or always greater than d, when the water is violently accelerated and the block receives a violent retarding impulse as it strikes the water surface. Also, since the first wave is a shallow water wave, which has properties determined by the water depth, the parameter $\frac{y_{smax}}{h}$ seems a strange choice.

Generally there is not much correlation between the Weigel et al study and this study. One possible explanation is the slight difference in the experimental set-up mentioned earlier, but efforts to correlate data are frustrated by the lack of generality resulting from their rather poorly chosen parameters.

CHAPTER 3

BACKGROUND TO PRESENT STUDY

In October 1963 the colossal and well documented landslide into the reservoir behind the Vaiont Dam in Northern Italy occurred. The disaster caused the Ministry of Works to examine critically the possibility of rapid landslides into lakes and reservoirs or potential reservoir sites in New Zealand.

Interest centred primarily on conditions at the Matahina hydro-electric power station in the Bay of Plenty. The station augments the power supply to a paper mill some miles downstream of the dam, and to other industries and towns in the area.

The earth dam at the station is 200 ft. high and 1,200 ft. long. The area of lake adjacent to the dam is surrounded by a 300 ft. deep columnar-jointed volcanic flow extending for several miles along both sides of the lake (see Fig. 3.1). At a point close to the dam the base of the volcanic flow is 150 ft. above the lake level.

A large earthquake could possibly dislodge several thousand cubic yards of the columnar flow from the cliffs into the lake, causing large surface waves to advance towards

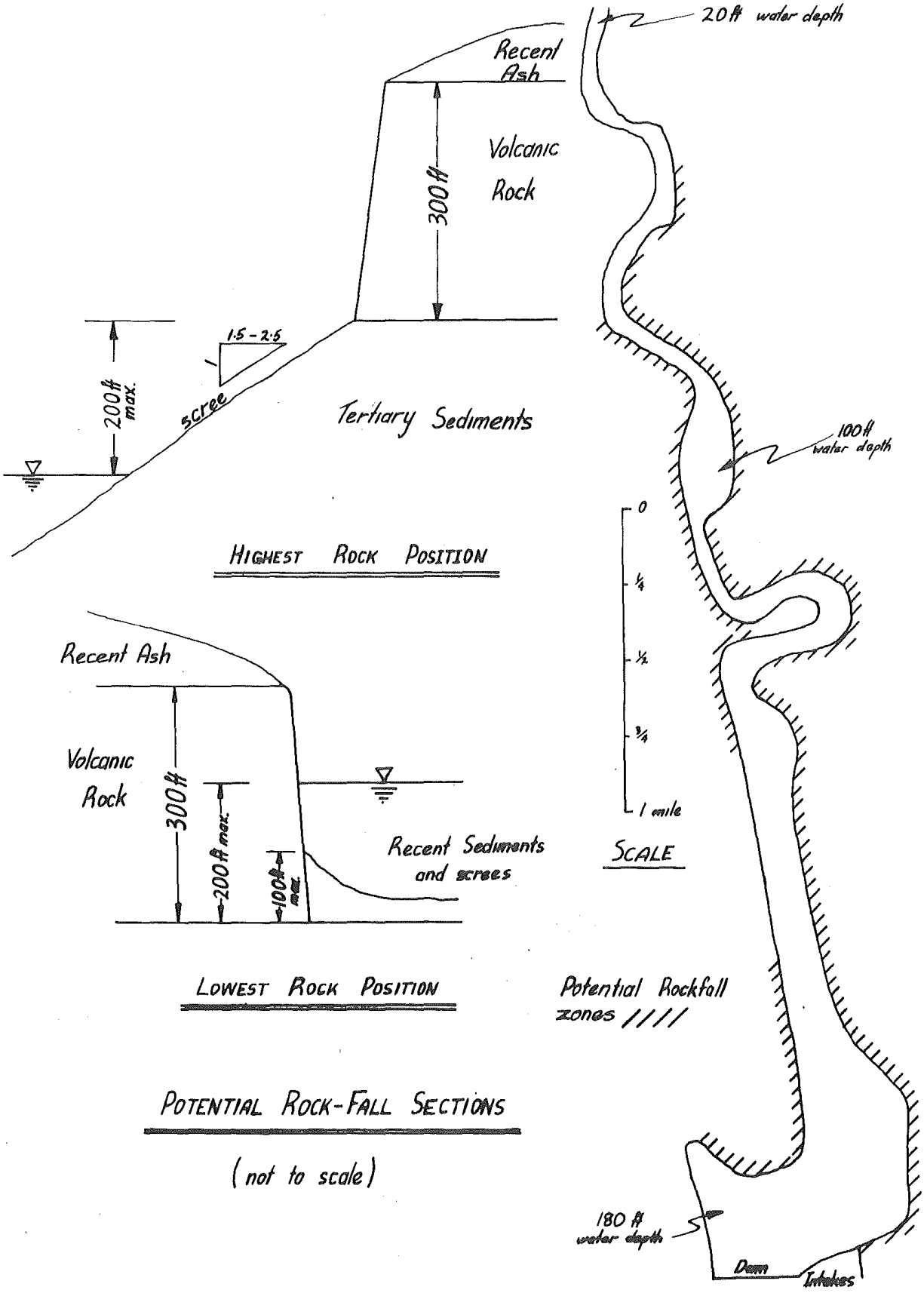

POTENTIAL ROCK-FALL SECTIONS

(not to scale)

Fig. 3.1 APPROXIMATE PLAN OF MATAHINA RESERVOIR

the dam. Any overtopping might easily cause catastrophic failure of the dam and extensive flooding of the very flat plains below the dam site.

The Ministry of Works asked Professor F.M. Henderson, formerly of the University of Canterbury, to estimate the possible effects of a landslide into the reservoir. He assumed that the displacement of water caused by a landslide could be modelled by the horizontal movement of a vertical wall at one end of a channel. The surge resulting from the forward motion of the wall would continue until the negative wave, formed when the wall stopped, caused the surge to subside.

Nevertheless, Professor Henderson considered that an experimental study would avoid the sweeping assumptions of such a model and provide a more satisfactory approach to the problem. An elementary experimental study was started under the direction of Professor Henderson. The desire for a detailed study resulted in this thesis being undertaken, under the direction of Mr. R.F. Hince, Senior Lecturer at the University of Canterbury.

CHAPTER 4

EXPERIMENTAL SET-UP

The 100 ft. long steel flume in the University of Canterbury Fluid Mechanics Laboratory made an ideal horizontal two-dimensional channel for this experimental study. The channel was 24 inches wide and could be filled to a maximum water depth of 23 ins.

A block dropping structure was constructed and mounted at one end of the flume. Detailed drawings appear in Appendix I. The dropping structure was designed to drop blocks, weighing up to 500 lb., freely into water.

A large tension spring mounted on the dropping structure was attached by an interconnecting chain to the block. The spring (k=224 lb/in) quickly and gently stopped the block before it hit the channel floor with an impulse which was assumed to act instantaneously. A non-return brake (see Fig. AI.5) attached to the spring prevented motion in the reverse direction. Varying the length of the chain varied the height at which the block stopped after entering the water.

The main reason for controlling the depth to which a block fell was that this distance is an important parameter in its own right. Another reason was to prevent damage to the channel floor. Pressures underneath the falling block

could reach 1,000 lb/ft^2 with the equipment described. If the block was allowed to fall freely to the floor, pressures could be considerably greater.

The blocks used were hollow steel boxes which could be loaded to give various densities. Their fall was guided by the heavy duty steam pipe shafts of the dropping structure. Wheels were used to reduce losses by lowering friction between the blocks and the shafts. Three block sizes were used, all being 23¼" wide, with cross-sections:

(a) 12.0" long x 12.8" high

(b) 9.5" long x 8.3" high

(c) 19.0" long x 8.3" high

A backing board across the channel and just behind the dropping structure simulated a lake wall and provided one-directional flow. The distance between the block and backboard could be varied over a range of approximately 11 inches. The backing board could also be removed to allow flow in both directions. This simulates a block of half the length dropping into the channel with no gap between backboard and block.

A continuous record of wave heights at several points down the channel was desirable. As the waves passed four points along the channel, the variations in conduction across partially submerged pairs of parallel brass rods were measured

by Phillips PR9304 electronic bridges. The outputs of the bridges were fed into a Phillips PT2108 oscilloscript which traced a continuous permanent record of the wave on paper.

Experimental Technique

The experimental technique is not germane to the main text and is therefore placed in Appendix II.

CHAPTER 5

DIMENSIONAL ANALYSIS

The development of a solution to the rockfall problem from the basic equations of fluid motion is thought to be a very difficult, if not impossible, problem. The development of an experimentally derived solution is the obvious area for research.

Of the waves generated by a falling block, the leading, or first crest was usually the largest, and subsided less than the waves in the wave train. Thus even if the extended deep water wave train initially contained the highest wave generated, its rate of subsidence was sufficiently great that before long the shallow water first wave had become the highest.

Because the first wave is a shallow-water wave, there are substantial velocities and excess pressures present in the whole region underneath the crest. This first wave is most likely to damage the shoreline and structures on the shoreline of a reservoir. The damage caused by a large shallow water wave in Lituya Bay, Alaska after an earthquake on 9th July 1958, can easily be ascertained from Miller's observations [7].

This thesis is therefore primarily an investigation of properties of the first wave. Buckingham's theorem [5]

is the basis of the experimental study. This theorem states that if a situation is governed by n variables in m dimensions (e.g. length, time, mass) then n-m dimensionless parameters can be formed into an equation which uniquely describes the situation.

For the rock fall problem (Fig. 5.1) the following variables are considered important in defining the waves generated by a block falling into a channel.

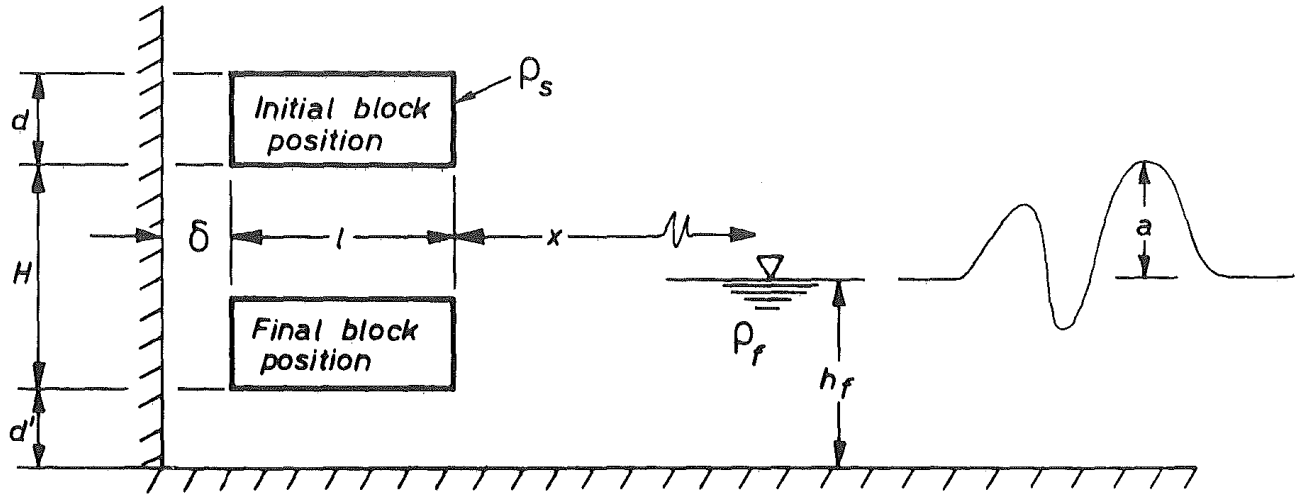

Fig. 5.1 The Rock Fall problem

The variables are defined as follows:

ρ_s = density of block,

ρ_f = density of water,

l = length of block,

d = height of block,

h_f = water depth,

a = first wave height,

δ = distance between end of channel and back of block,

d' = distance between bottom of fallen block and bottom of channel,

H = height through which the block falls,

x = distance along the channel from face of block.

There are ten variables in two dimensions, length and mass. Thus eight dimensionless parameters are required to form the terms of an equation which describes the motion. These parameters are all in terms of the two variables ρ_f and h_f which by themselves define any long two-dimensional channel.

$\frac{\rho_s}{\rho_f}$ = density of block: density of water ratio,

$\frac{l}{h_f}$ = length of block: water depth ratio,

$\frac{x}{h_f}$ = distance along channel: water depth ratio,

$\frac{d'}{h_f}$ = distance between bottom of fallen block and bottom of channel: water depth ratio,

$\frac{\delta}{h_f}$ = distance between back of block and back of channel: water depth ratio,

$\frac{H}{h_f}$ = fall height of block: water depth ratio,

$\frac{d}{h_f}$ = height of block: water depth ratio,

$\frac{a}{h_f}$ = first wave height: water depth ratio.

At this stage the reasoning behind the absence of any parameter involving a time dimension must be given.

Usually in a study of surface or gravity waves there is a gravity term involved in a description of the situation. In this case, however, the influence of gravity on the first wave properties (e.g. speed, energy) is identical to its influence on the block properties. Thus a time dimension need not be included in a description of the generation of the first wave, provided a description of a maximum wave height in terms of distance is considered sufficient.

Certain conditions do have to be met for this description to be valid. One condition is that the first wave must be non-oscillatory. Fortunately this is the case.

The second condition is that wave energy losses, which are velocity dependent, can be neglected. For large unbroken wave amplitudes the major cause of subsidence of first wave heights as they travel along the channel was

probably due to losses. However their subsidences were much less than the subsidence due to energy losses for solitary waves calculated from a formula derived by Keulegan [6].

$$\left(\frac{a}{h_f}\right)^{-\frac{1}{4}} - \left(\frac{a_o}{h_f}\right)^{-\frac{1}{4}} = \frac{1}{12}\left(1 + \frac{2h_f}{B}\right)\left(\frac{\nu^2}{gh_f^3}\right)^{\frac{1}{4}} \cdot \frac{x}{h_f}$$

where terms are:

a_o = wave height at a certain point in channel,

a = wave height at distance x along channel, from point where a_o is measured,

h_f = water depth,

B = width of channel,

g = acceleration due to gravity,

ν = kinetic viscosity of water,

x = distance along channel.

For an initial value $\frac{a_o}{h_f} = 0.500$ for a solitary wave in a channel 12" deep and 24" wide, the above expression yields a wave height of $\frac{a}{h_f} = 0.393$ at a distance of $x = 30\,h_f$ from the point where a_o was measured. This reduction of 21% in wave height due to losses is much greater than the typical 8% observed reduction in wave height over the same distance from the same size initial wave.

Even though losses may be assumed to cause most of the subsidence of a large unbroken wave, damage caused by such a wave will be catastrophic no matter whether losses exist or

not. Thus unless the height of such a wave is required at a point several hundred water depths away from the rockfall area, the extent to which losses affect subsidence of a large wave is an academic point.

It was found that the smaller the wave, the greater the subsidence. For wave heights of the order of $\frac{a}{h_f} = 0.25$ or less, the effect of losses was assumed to be negligible, the major cause of subsidence being due to the asymmetrical waveshapes.

Although the parameters are not very useful in their simplest form, certain modifications to them allow the situation to be described more readily. A close look at the mechanism of wave generation will explain the reasoning for these modifications. The mechanism can be roughly divided into three sections:

(a) The generation of an unstable hump of water in front of the falling block.

(b) The collapse of the hump causing one wave to proceed along the channel and another wave to collapse against the fallen block.

(c) The subsidence of the wave proceeding along the channel.

Photos. 6.1 to 6.8 show that as a block falls into the channel a large hump of water forms a small distance

in front of the block. At this stage the front face of the block is usually quite dry. Also, although it is hard to say for certain, it is probably that the back face of the block is dry. Thus the only surface of the block touching water is its bottom face.

This strikes the water surface at a velocity determined by the initial height of the block. From Fig. 5.1 it is seen that this height is $H + d' - h_f$ above the water surface, or $H + d'$ above the channel floor. Thus, relating the height to the water depth, a parameter $\frac{H + d'}{h_f}$ can be formed which relates the initial height of the block above the channel floor to the water depth.

As the bottom face of the block strikes the water surface, all the water under the block is set in motion. A measure of the amount of water set in motion is thus $\frac{1}{h_f}$.

As the block falls into the water, considerable pressures are induced underneath the block to push the water out either of the escape routes - horizontally from under the front of the block or upward through the gap between the block and the channel wall. These pressures also act on the block against the downward forces of gravity, to eventually decelerate the box. The downward force per unit length of block is related to the quantity $\rho_s d$. Making this term dimensionless, a parameter $\frac{\rho_s d}{\rho_f h_f}$ is formed, and is termed the mass flux ratio.

A measure of the excape paths for water underneath the falling block is $\frac{\delta}{h_f}$ and the parameter $\frac{d'}{h_f}$ determines the extent to which water is displaced by the block.

The five parameters $\frac{H+d'}{h_f}$, $\frac{l}{h_f}$, $\frac{\rho_s d}{\rho_f h_f}$, $\frac{\delta}{h_f}$, and $\frac{d'}{h_f}$ are thought to describe completely the formation of the hump. As the hump collapses some of these become unimportant.

Assuming the block does not move again once it has ceased motion (one condition being that the block density ρ_s is greater than the water density ρ_f), the parameter $\frac{\rho_s d}{\rho_f h_f}$ will cease to affect the wave motion. Similarly $\frac{H+d'}{h_f}$ having determined the characteristics of the hump, will not affect its collapse.

Consider the situation as the hump collapses back against the block (Fig. 5.2). As the hump strikes the block the heights $d + d'$ and d' become important. The height of $d+d'$ determines the fraction of the hump that can collapse over the block, and despite the experimental results below, it is thought to be important in the generation of the first negative wave. The height d', combined with the values of δ and l, determines the amount of water in the collapsing hump that can escape through the "elbow bend" under the block and up the space between the channel wall and the back of the block.

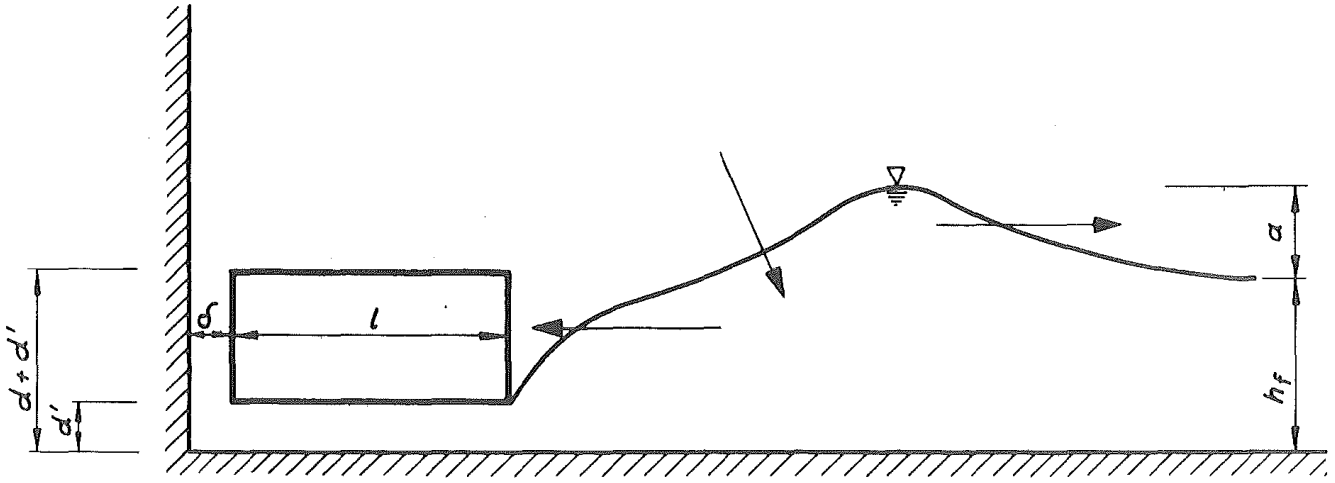

Fig. 5.2
Collapse of hump

Between them, the parameters $\frac{d+d'}{h_f}$, $\frac{d'}{h_f}$, $\frac{\delta}{h_f}$, and $\frac{l}{h_f}$ influence the manner in which the hump collapses and forms the negative wave. This negative wave would seem to be the major reason for the first wave's subsidence. As they proceed along the channel, both the first wave and first trough gradually diminish in amplitude At this stage, the distance along the channel $\frac{x}{h_f}$ becomes important in defining $\frac{a}{h_f}$.

Thus the rockfall problem is assumed to be adequately described by the function

$$\frac{a}{h_f} = f\left(\frac{l}{h_f}, \frac{\rho_s d}{\rho_f h_f}, \frac{H+d'}{h_f}, \frac{\delta}{h_f}, \frac{d'}{h_f}, \frac{d+d'}{h_f}, \frac{x}{h_f}\right) .$$

CHAPTER 6

RESULTS

In all cases where a block fell vertically into water, the water displaced by the falling block formed a hump in front of the block, as shown in Photos. 6.1 to 6.8.

The far channel wall shown in these photographs has a 3 inch square grid marked on it. Information on the parameters involved for the photographed runs is shown in Table 6.1.

In most runs studied, the front face of the falling block was dry, indicating that the volume of water initially displaced is usually greater than the volume of the block. Note Photo. 6.8 where there is a distance of over 9 inches between the block front and the water surface.

A sequence of frames taken at roughly 0.1 sec. intervals showing the 12.0" x 12.8" block falling into water 19.6" deep is shown in Photos. 6.9 to 6.34.

When the block strikes the water surface it is retarded suddenly (viz. Photos. 6.9 to 6.13) and the water is violently accelerated forwards and upwards from under the block (Photo. 6.13). The block continues falling till it finally comes to rest in Photo 6.15. By the time 0.4 sec. (Photo 6.16) have elapsed

TABLE 6.1

Photo No.	$\frac{l}{h_f}$	$\frac{\rho_s d}{\rho_f h_f}$	$\frac{H+d'}{h_f}$	$\frac{\delta}{h_f}$	$\frac{d'}{h_f}$	$\frac{d+d'}{h_f}$	$\frac{a}{h_f}$*
6.1	0.61	1.30	1.28	0.08	0.21	0.86	0.4
6.2	0.61	1.30	1.89	0.08	0.18	0.83	0.6
6.3	0.61	1.30	2.39	0.08	0.16	0.81	0.7
6.4	0.69	1.47	2.70	0.09	0.18	0.92	0.75
6.5	0.69	1.47	2.08	0.09	0.20	0.94	0.7
6.6	0.69	1.47	1.31	0.09	0.22	0.96	0.5
6.7	0.76	1.62	1.36	0.10	0.25	1.06	0.6
6.8	0.76	1.62	2.90	0.10	0.18	0.99	0.8

* These values of $\frac{a}{h_f}$ are the approximate maximum wave heights in the region of the block.

Maximum Wave Heights in the vicinity of the block

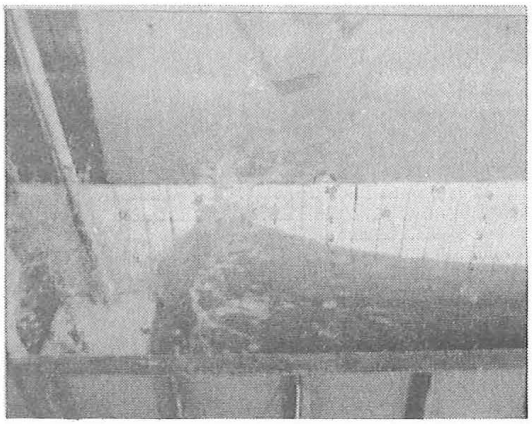

fig 6.1

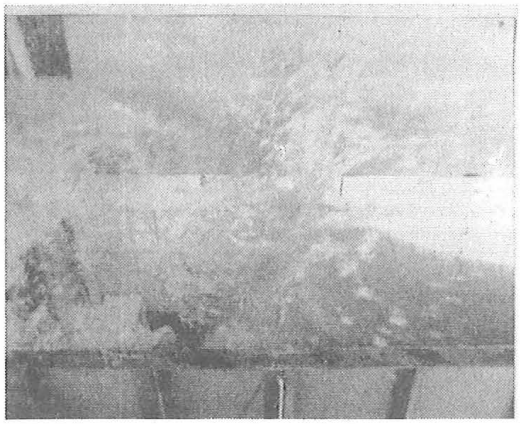

fig 6.4

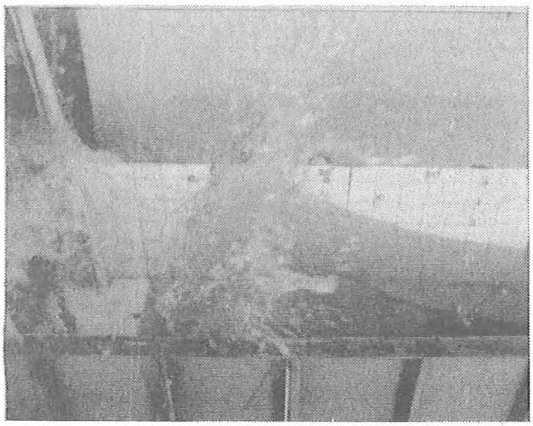

fig 6.2

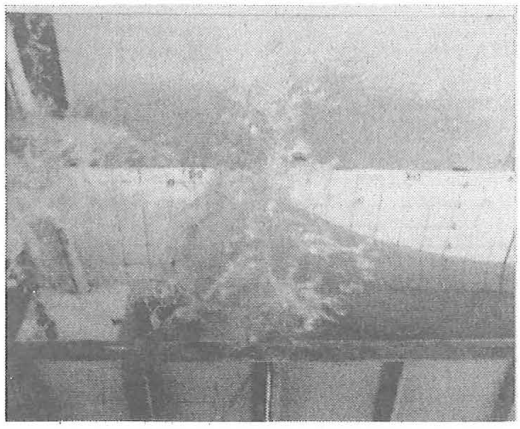

fig 6.5

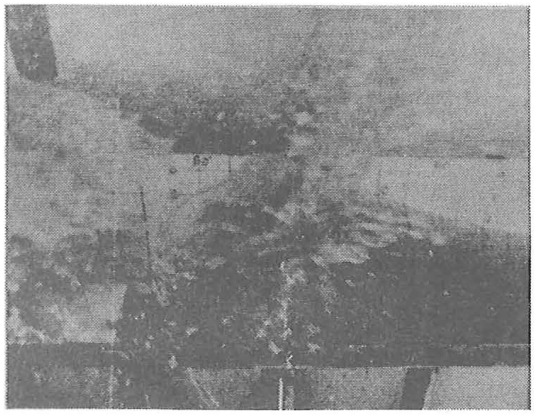

fig 6.3

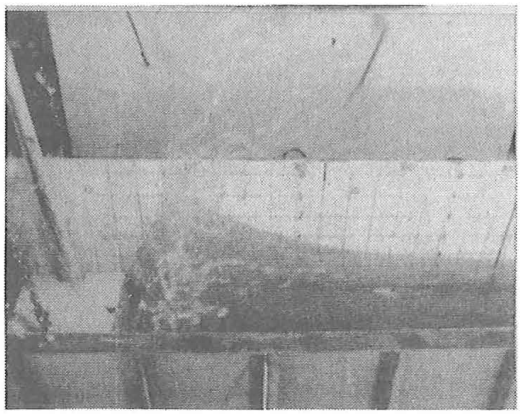

fig 6.6

Maximum Wave Heights in the vicinity of the block (cont.)

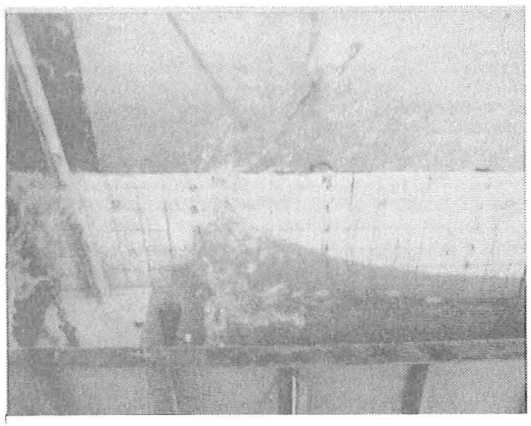

fig 6·7

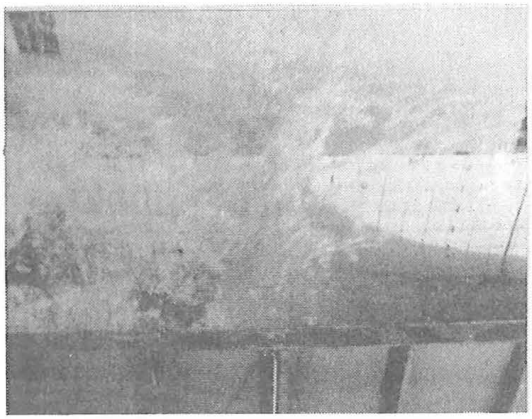

fig 6·8

Sequence for Run 3 (Frame Intervals approx. 0·1 sec.)

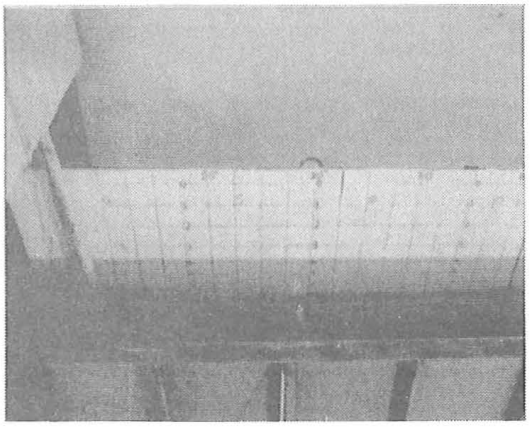

fig 6·9

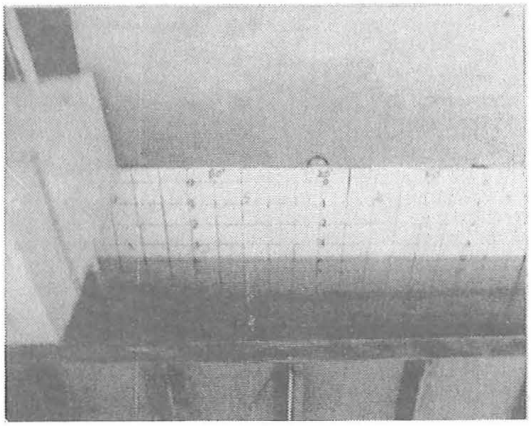

fig 6·11

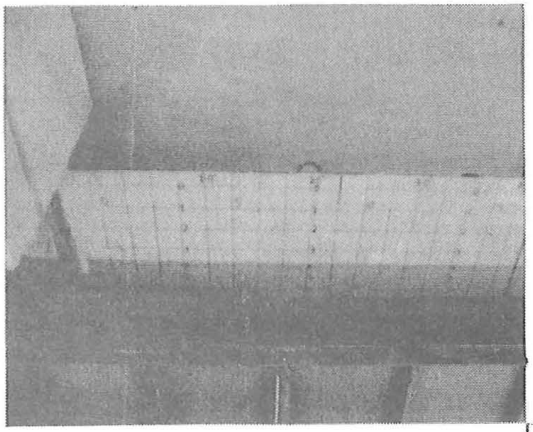

fig 6·10

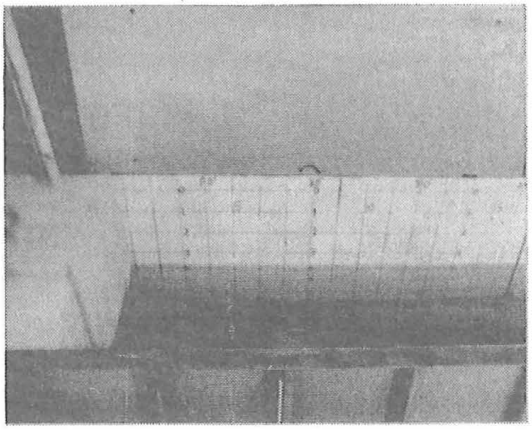

fig 6·12.

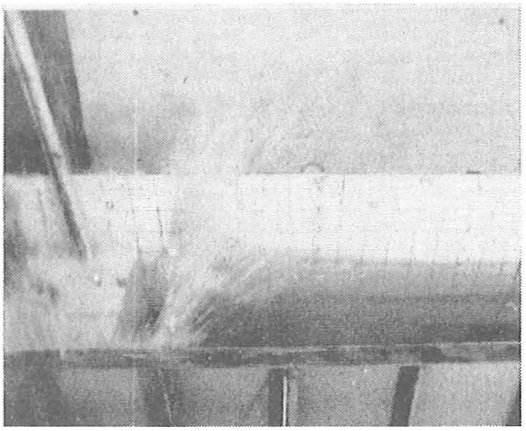

fig 6·13

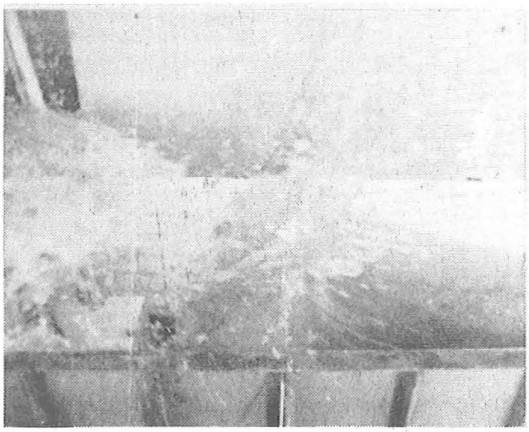

fig 6·16

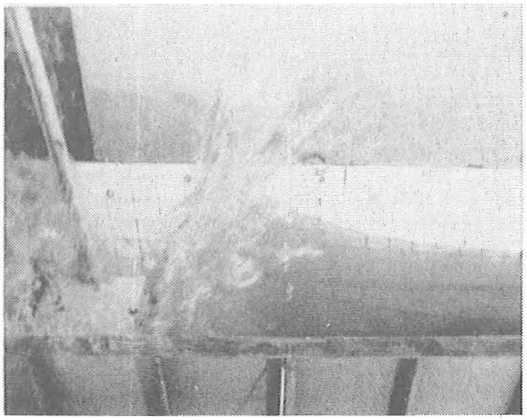

fig 6·14

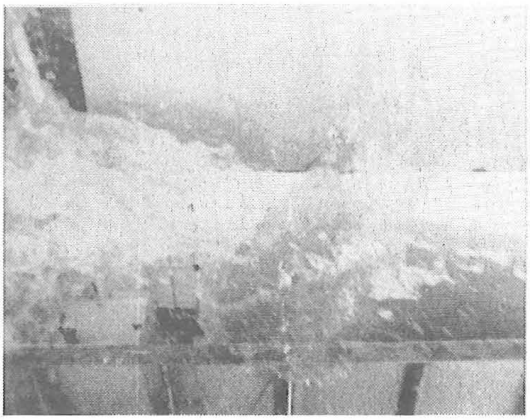

fig 6·17.

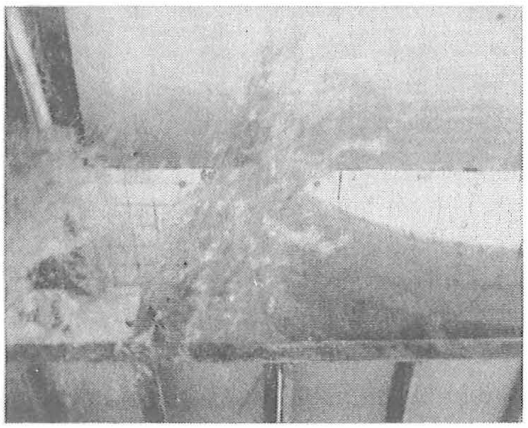

fig 6·15

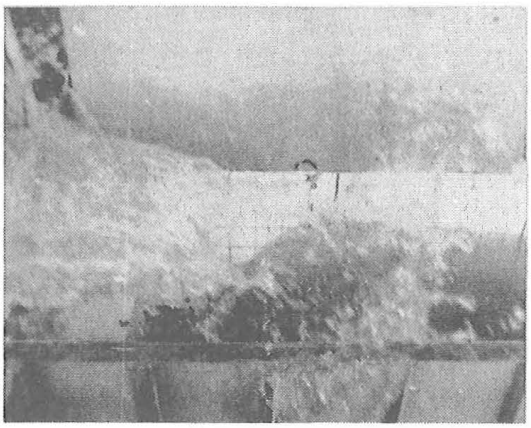

fig 6·18

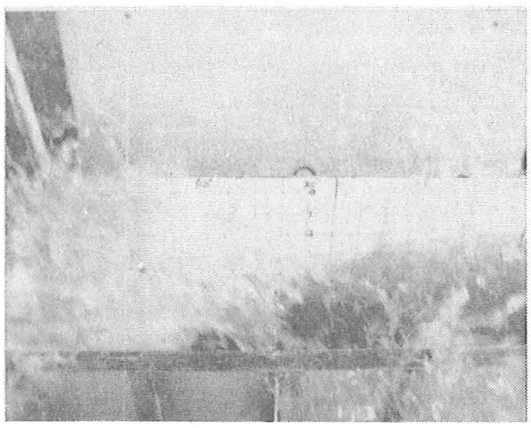

fig 6·19

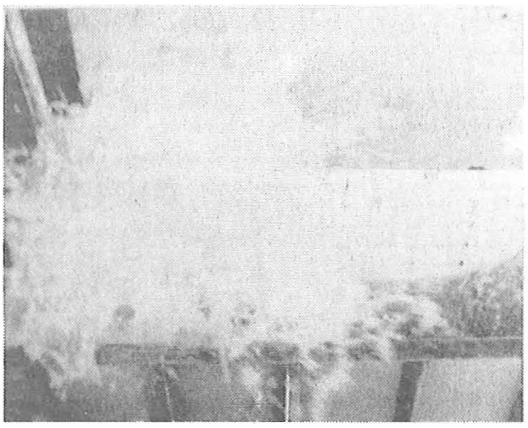

fig 6·22.

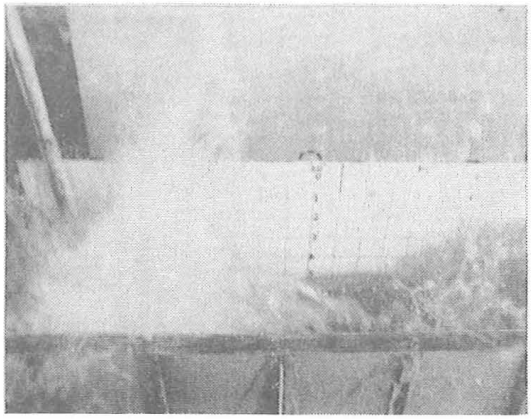

fig 6·20

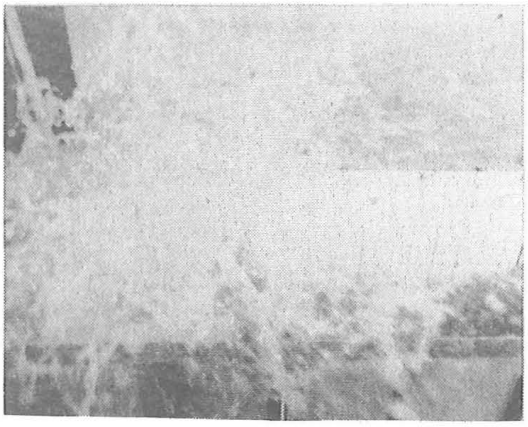

fig 6·23

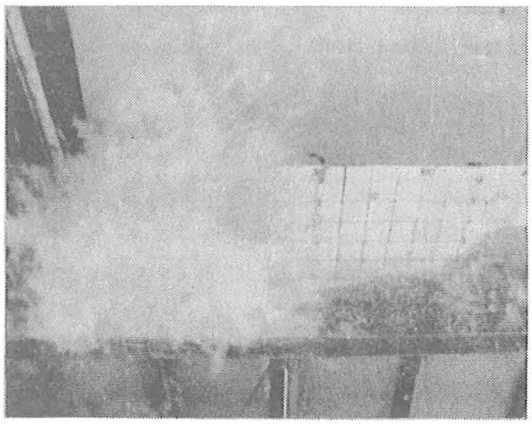

fig 6·21

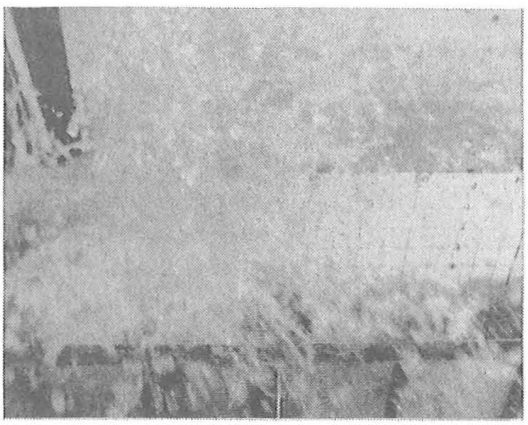

fig 6·24

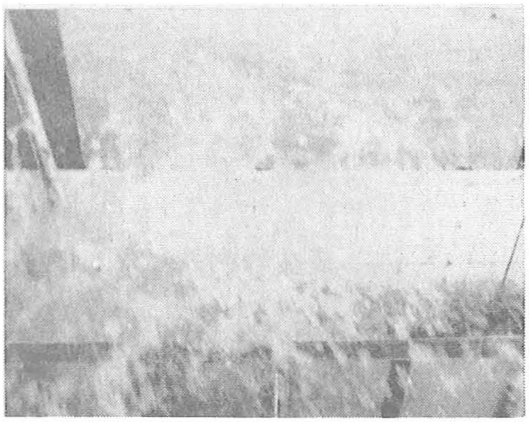

fig 6.25

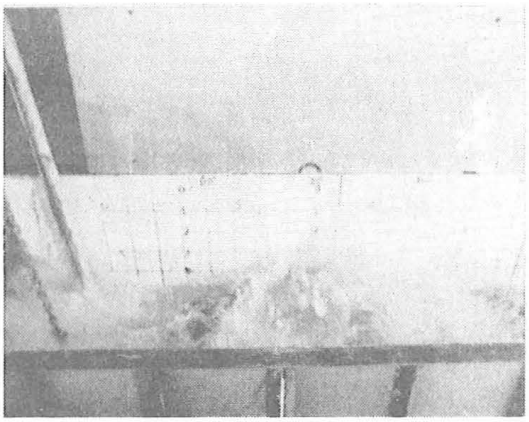

fig 6.28

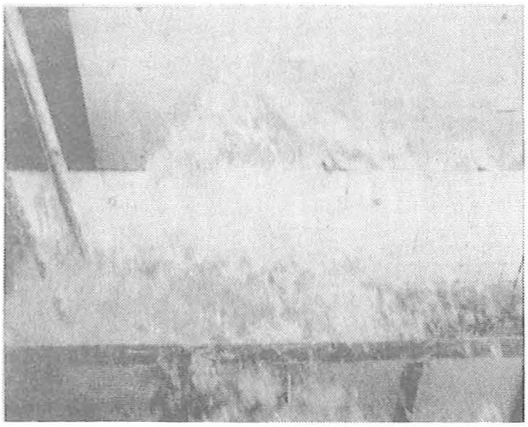

fig 6.26

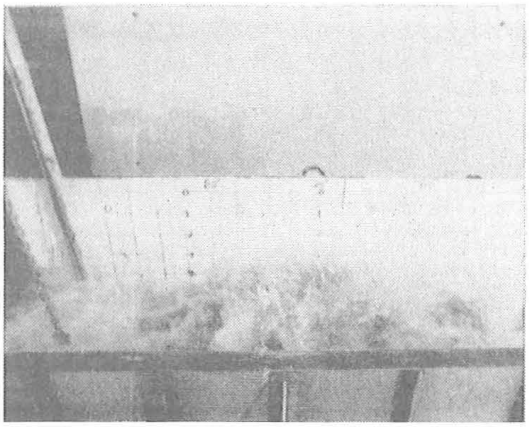

fig 6.29

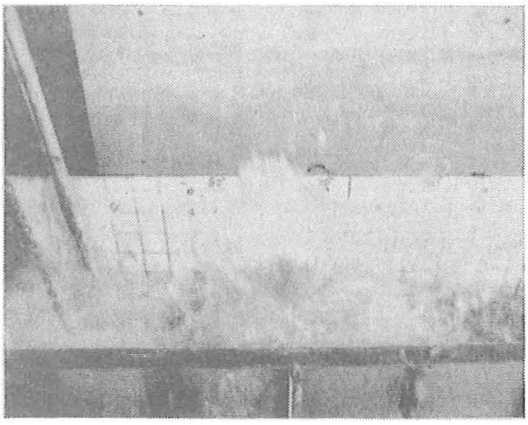

fig 6.27

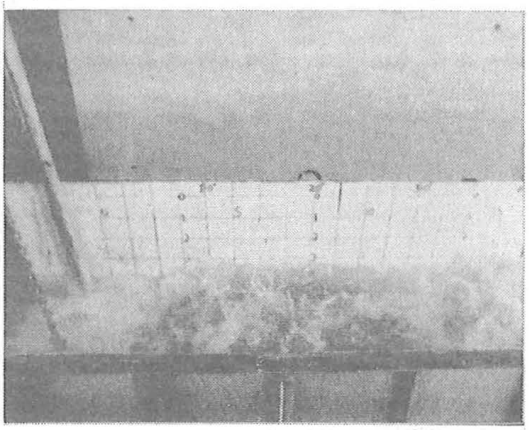

fig 6.30

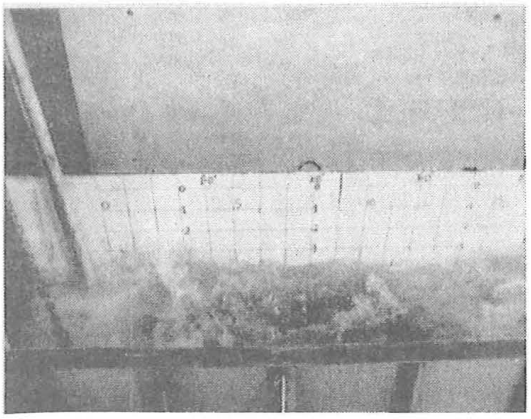

fig 6·31

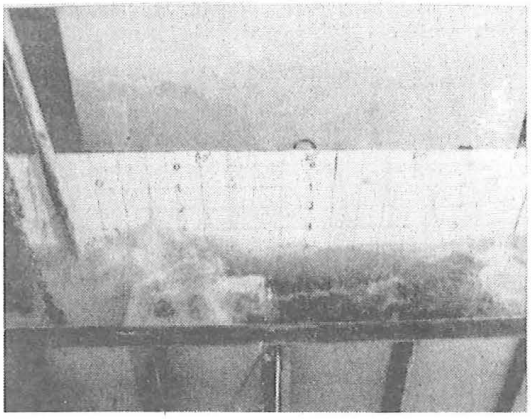

fig 6·33

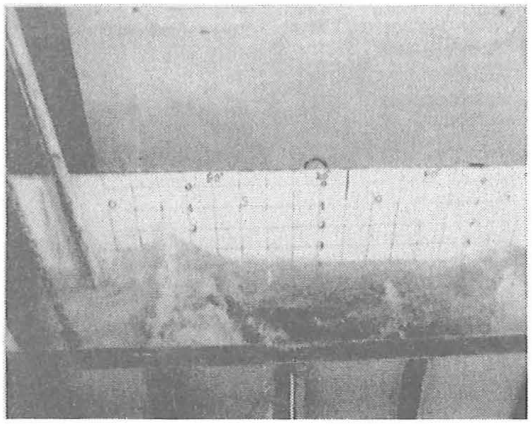

fig 6·32.

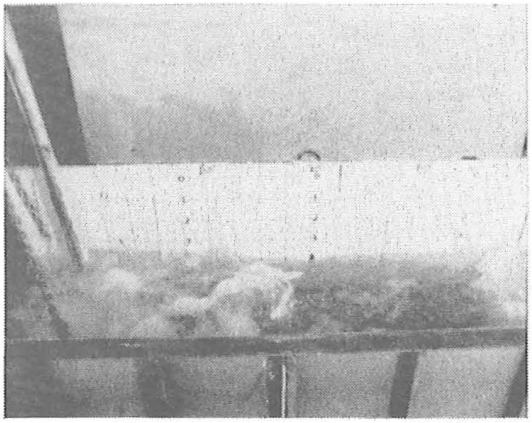

fig 6·34.

since block impact, the water has reached the top of the channel wall. The hump then begins to collapse, even though most of the water is still moving forward. After 0.8 secs. the hump has subsided from over 13 inches high (Photo. 6.16) to about 6 inches high (Photo.6.20) and is quickly moving to the right, out of the field of the photograph.

Some water escapes from under the block by passing through the gap between the back of the block and the back board. This water is first obvious in Photo. 6.14, 0.2 secs. after impact. It reaches a maximum height in Photos. 6.16 or 6.17 then starts collapsing. There is an appreciable horizontal velocity in this water and by Photo 6.19, at 0.7 secs., it has arched over the block and covered a distance of over 2 ft. 6 in. from the back of the block.

Although up until 0.7 secs., after impact (Photo.6.19) most water seems to be moving forward, the near vertical rear face of the hump, so evident in Photo. 6.16, is collapsing from the bottom. This water accelerates rapidly back onto the front face of the block. hitting it with some violence (Photo. 6.20). Photos. 6.22 and 6.23 show that the water from this splash has reached a height of about 3 or 4 feet above the still water surface.

The water surface behind the hump and in front of the splash zone from Photo. 6.20 to 6.28, 0.8 to 1.6 seconds after impact, is seen to be roughly horizontal about 3 inches below the still water level. As the water ejected vertically on impact with the block collapses (Photo 6.31, 1.9 sec., after impact) and by Photo 6.34, 2.2 secs. after impact, the water level is roughly horizontal and close to the original still water level.

The repeated formation and collapse of these waves in the vicinity of the block is thought to be the prime reason for the formation of an extended deep water wave train which followed the first wave along the channel. The whole disturbance as it travelled along the channel is of the form depicted in Fig. 6.35.

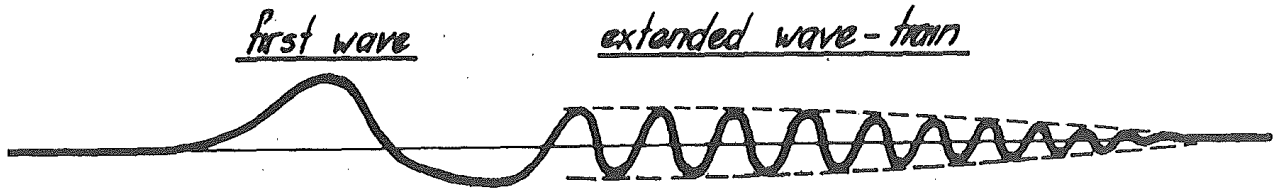

Fig. 6.35
Typical form of waves travelling along the channel

As the waves travelled away from the region of the block, the faster first wave tended to separate from the oscillatory wave train. The front of the oscillatory wave train travelled at a speed of the order of three times the speed of the tail of the wave train, thus the wave train became very long within a short time.

CHAPTER 7

DISCUSSION OF RESULTS

The discussion of results is divided into the following sections:

A. The generation of the large hump of water in front of the falling block.

B. The collapse of the hump, both away from the block and back onto the block.

C. The subsidence of the wave as it travels along the channel.

Section A. The generation of the large hump of water in front of the falling block

As a block falls through air towards the water, it accelerates under gravity, and when it reaches the water surface its velocity V_o is given by

$$V_o = (2gh)^{\frac{1}{2}}$$

where h is the free fall height of the block. On striking the water surface the block receives a violent retarding impulse, and the water under the block is violently accelerated. This initial acceleration is assumed to be caused by a compression wave spreading through the water from the bottom of the block. Since the velocities of the block and the water are so very small (up to 25 ft/sec) compared

with the velocity of a compression wave through the water (4720 ft/sec), it seems reasonable to assume that energy losses as the block enters the water will be small enough to be considered negligible. Thus the energy of the block just before it strikes the water surface can be equated with the energy of the block and water just as the block touches the water as shown in Fig. 7.1. (Assume that there is no gap between the block and the back board.)

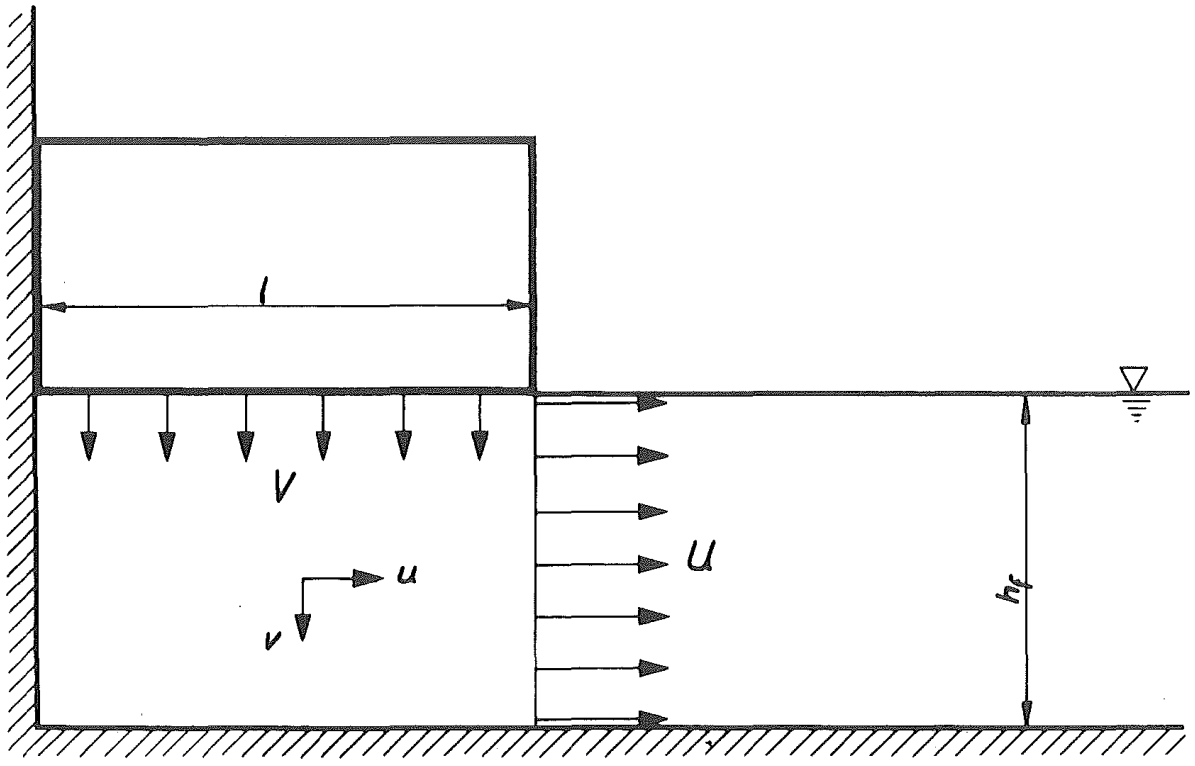

Fig. 7.1

Situation as the block strikes the water surface.

Assume that the horizontal velocity across any vertical section is constant,

i.e. assume $u = \frac{x}{l} \cdot U$

and similarly assume $v = \frac{y}{h_f} \cdot V$.

Then, equating the kinetic energies before and after impact,

$$\frac{1}{2}\rho_s d1 V_o^2 = \frac{1}{2}\rho_s d1 V^2 + \frac{1}{2}\rho_f \int_A (u^2 + v^2) dA$$

$$= \frac{1}{2}\rho_s d1 V^2 + \frac{1}{2}\rho_f \int_0^{h_f} \int_0^{1} \left(\left(\frac{U.x}{l}\right)^2 + \left(\frac{V.y}{h_f}\right)^2 \right) dx.dy$$

By continuity $U.h_f = V.1$

thus

$$\frac{1}{2}\rho_s d1 V_o^2 = \frac{1}{2}\rho_s d1 V^2 + \frac{1}{2}\rho_f V^2 \int_0^{h_f} \int_0^{1} \left(\frac{x^2}{h_f^2} + \frac{y^2}{h_f^2}\right) dx.dy$$

whence the block velocity V is given by:

$$\frac{V^2}{V_o^2} = \left(1 + \frac{\rho_f h_f}{3\rho_s d} \left(\frac{1^2}{h_f^2} + 1\right)\right)^{-1} \qquad \ldots \quad (1)$$

and the water velocity under the front of the box is given by:

$$\frac{U^2}{V_o^2} = \frac{1^2}{h_f^2} \left(1 + \frac{\rho_f h_f}{3\rho_s d} \left(\frac{1^2}{h_f^2} + 1\right)\right)^{-1}$$

The assumptions that the above is approximately true are that the motion of water under the block is not significantly affected by the water in the channel in front of the

block and that $\frac{l}{h_f}$ is sufficiently large that the horizontal water velocity across any cross-section is constant. Probably this is so if $\frac{l}{h_f}$ is greater than about 3. For values less than 3, there presumably exists a transitional region where the water velocity along the bottom of the channel is slower than that along the bottom of the block. At some stage, possibly around $\frac{l}{h_f} = 0.3$, the water at the bottom of the channel remains ostensibly at rest as the block penetrates the water surface. Effectively the block is falling into deep water.

In terms of the above reasoning this study is confined to most of the transitional range.

Even though this study is not related to the range of large $\frac{l}{h_f}$, it is interesting to note the effects that parameters $\frac{l}{h_f}$ and $\frac{\rho_s d}{\rho_f h_f}$ have on the block-water mechanics when $\frac{l}{h_f}$ is large. Since $\frac{l}{h_f}$ is large, equation (1) becomes

$$\frac{V^2}{V_o^2} = \left(1 + \frac{\rho_f h_f}{3\rho_s d} \cdot \frac{l^2}{h_f^2}\right)^{-1}$$

As $\frac{l}{h_f}$ increases, the impulse the block receives increases and the velocity of the block after entry is reduced. Also, if the mass flux ratio $\frac{\rho_s d}{\rho_f h_f}$ is increased, the impulse on the block is reduced and the velocity of the block after entry is raised.

The water velocity U is affected by $\frac{\rho_s d}{\rho_f h_f}$ in the same manner. However, it is not significantly affected by changes in $\frac{l}{h_f}$ for larger values of $\frac{l}{h_f}$.

The water velocity U, and the manner in which the falling block travels are the major quantities which affect the formation of the large hump of water in front of the block, and hence the formation of the first wave. The first wave height $\frac{a}{h_f}$ would be expected to be dependent on the same parameters that affect the water motion near the block, and to follow roughly similar trends as the values of the parameters change. Thus for small block lengths, the first wave height should be dependent on $\frac{l}{h_f}$ and $\frac{\rho_s d}{\rho_f h_f}$. For larger block lengths, $\frac{a}{h_f}$ should not be so dependent on $\frac{l}{h_f}$.

Results from the experimental study showed for values of $\frac{l}{h_f}$ of 1.53, 1.67, and 1.81, with respective values of $\frac{\rho_s d}{\rho_f h_f}$ of 1.45, 1.57 and 1.70 (i.e. runs 21-33, see Appendix III), that the first wave height was roughly independent of $\frac{l}{h_f}$. Other runs where $\frac{l}{h_f}$ was in the same range (i.e. runs 40-47 where $\frac{l}{h_f} = 1.65$) but with $\frac{\rho_s d}{\rho_f h_f}$ values of 2.20 and 2.65 indicated that the first wave height was dependent on $\frac{l}{h_f}$ thus following the pattern of results for the remainder of the experiments. This may be due in part to the reduction of the term in equation (1),

$(1+\frac{\rho_f h_f}{3\rho_s d}(\frac{l^2}{h_f^2}+1))^{-1}$ caused by the larger value of $\frac{\rho_s d}{\rho_f h_f}$.

Apart from the variations described for runs 21-33, the results of the experimental study showed that over the ranges tested the first wave height at $x = 10h_f$ could be simply described as being nearly linearly proportional to $\frac{1}{h_f}$ and $(\frac{\rho_s d}{\rho_f h_f})^{0.4}$ as shown in Fig. 7.2.

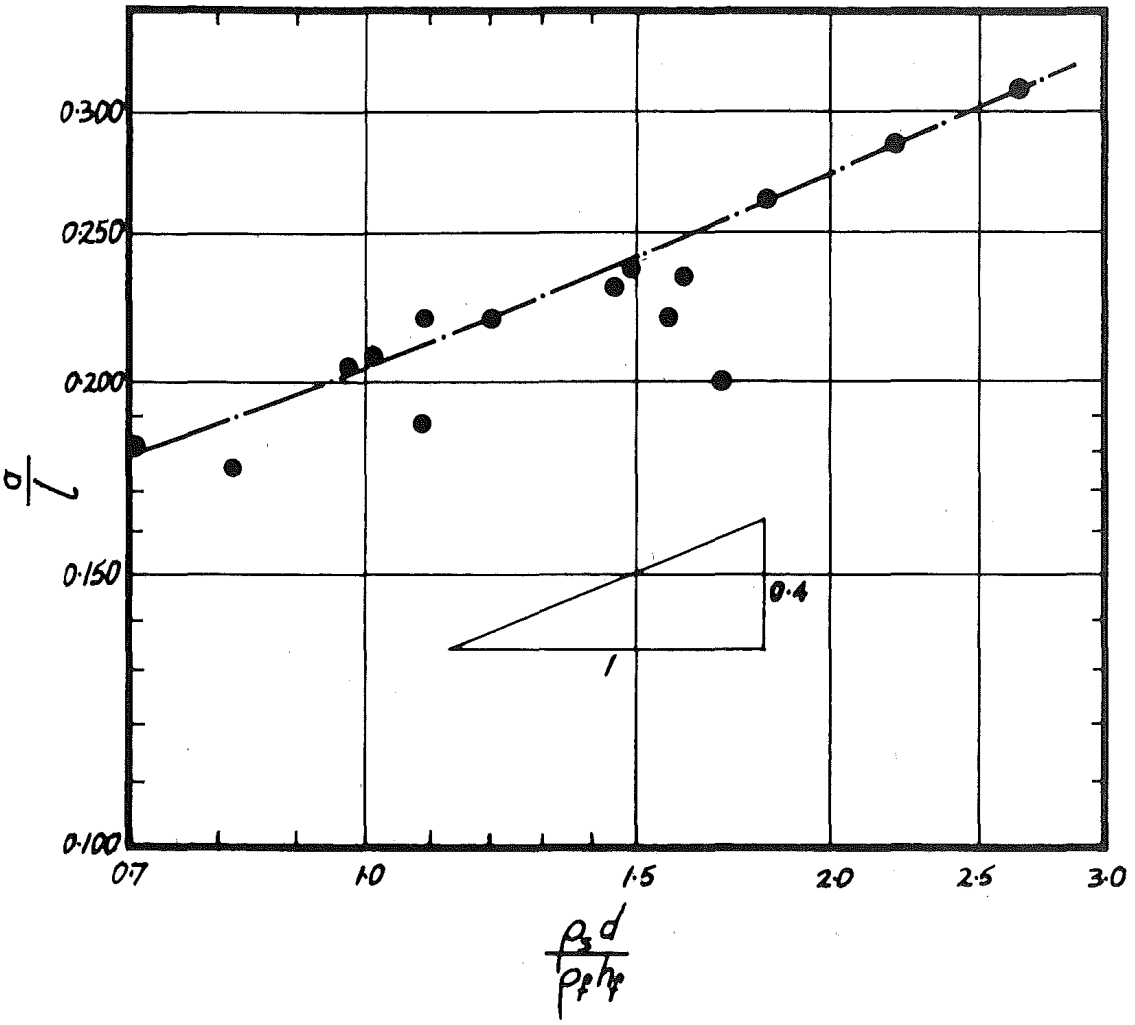

Fig. 7.2

Relationship between $\frac{a}{l}$ and $\frac{\rho_s d}{\rho_f h_f}$ for $\frac{H+d'}{h_f} = 1.00$; $\frac{\delta}{h_f} = 0$; $\frac{d'}{h_f} = 0$; $\frac{x}{h_f} = 10$

It is well appreciated that an equation of the sort

$$\frac{a}{h_f} = \frac{l}{h_f}\left(\frac{\rho_s d}{\rho_f h_f}\right)^{0.4} f\left(\frac{\delta}{h_f}, \frac{d'}{h_f}, \frac{d+d'}{h_f}, \frac{H+d'}{h_f}\right) \qquad \text{for } x = 10h_f$$

is not the exact solution to the rockfall problem. However, over the ranges

$$0.52 \leqslant \frac{l}{h_f} \leqslant 1.65$$

$$0.71 \leqslant \frac{\rho_s d}{\rho_f h_f} \leqslant 2.65$$

the above relationship is accurate to within a few per cent.

As could be expected, an increase in block fall height caused an increase in the first wave height. At a distance $x = 10h_f$ from the block, the first wave height could be expressed accurately in the form

$$\frac{a}{h_f} = \frac{l}{h_f}\left(\frac{\rho_s d}{\rho_f h_f}\right)^{0.4} \left(\frac{H+d'}{h_f}\right)^{n} \cdot f\left(\frac{\delta}{h_f}, \frac{d'}{h_f}, \frac{d+d'}{h_f}\right) \qquad \text{... (2)}$$

at $x = 10h_f$

for $1 \leqslant \frac{H+d'}{h_f} \leqslant 3.3$ where n was a constant determined by the value of $\frac{l}{h_f}$ and $\frac{\rho_s d}{\rho_f h_f}$.

The value of $\frac{H+d'}{h_f}$ determines the velocity at which the block strikes the water. Thus, in conjunction with $\frac{l}{h_f}$ and $\frac{\rho_s d}{\rho_f h_f}$, it determines the water velocities under the block, and the velocity of the block immediately after it has struck the water surface.

The value of n in equation (2) varied between about 0.5 and 1.1 over the range tested. The manner in which n is dependent on $\frac{l}{h_f}$ and $\frac{\rho_s d}{\rho_f h_f}$ was not very distinct as can be seen in Fig. 7.3. Although a trend could be seen, a quantitative relationship could not be found.

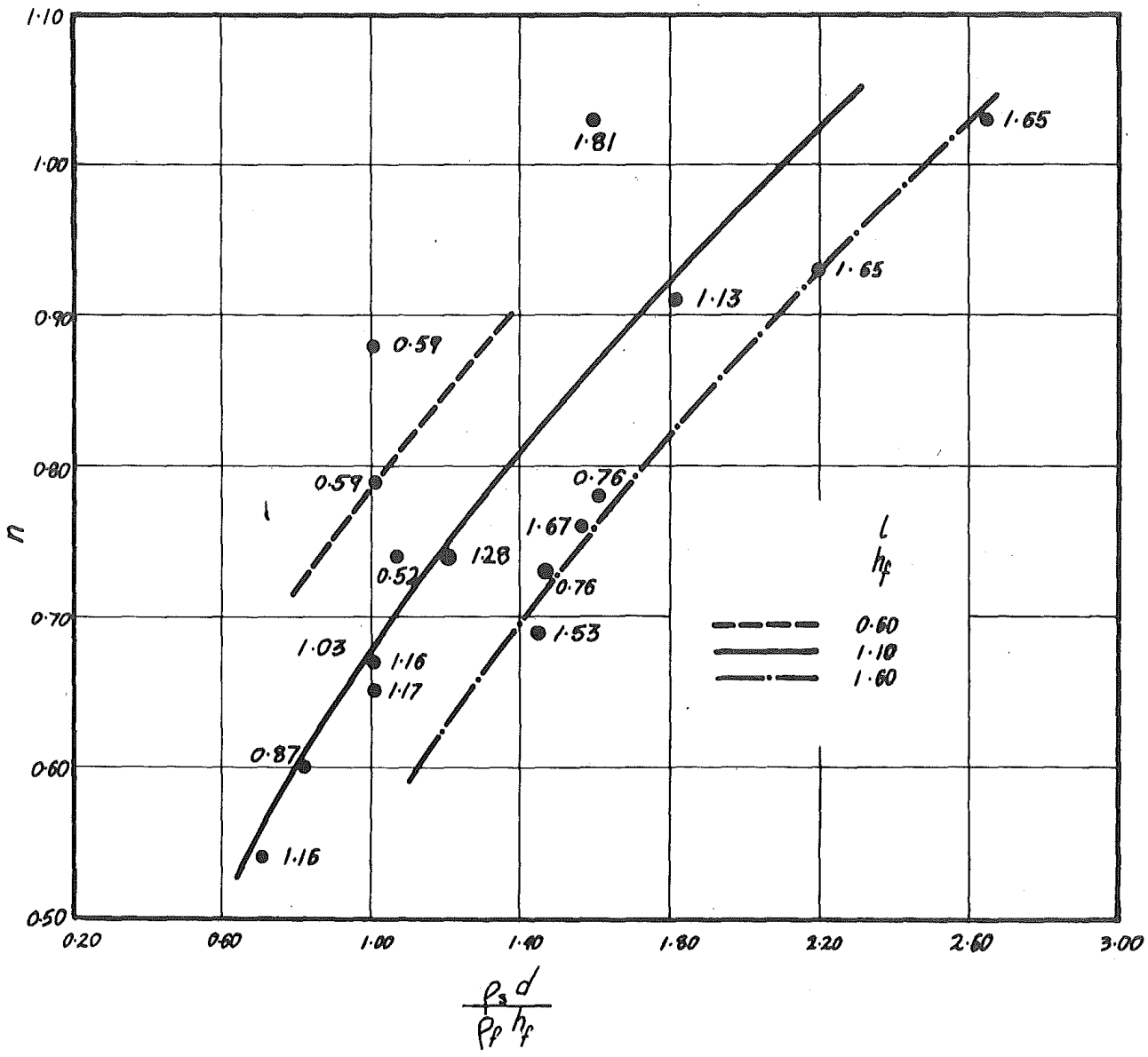

Fig. 7.3

Relationship between n (at $x = 10 h_f$) and $\frac{\rho_s d}{\rho_f h_f}$ for varying $\frac{l}{h_f}$. Values of $\frac{\delta}{h_f}$ and $\frac{d'}{h_f}$ are small and their effects are assumed to be of minor importance.

Qualitatively, the relationship can be explained as below. For a block with large $\frac{l}{h_f}$ and small $\frac{\rho_s d}{\rho_f h_f}$ it has been shown that block fall velocity is greatly reduced at the instant the block strikes the water surface. As well as this, the sum of the positive pressures along the underside of the block is large compared with the gravitational force acting on the block. Thus the block is soon decelerated and falls slowly through the water, causing a long, low hump in front of the block. Because the block is decelerated so quickly, the first wave height is not very dependent on the block fall height, and the value of n is low.

For a block with small $\frac{l}{h_f}$ and large $\frac{\rho_s d}{\rho_f h_f}$, the reduction in block fall velocity on entry into the water is much diminished. Also the pressure forces are smaller relative to the gravitation force, causing less deceleratiom of the block. Hence $\frac{a}{h_f}$ is much more dependent on the block fall height and the value of n is large accordingly.

The formulation given in equation (2) was found to hold for values of $\frac{a}{h_f}$ less than 0.63. Values greater than 0.63 gave broken bores, which behaved quite differently to the unbroken waves which this study concentrates on. Probably larger unbroken waves could be generated if the block length ratio $\frac{l}{h_f}$ was increased from the 1.81 maximum

used in this study to 5.0 or greater. Then values of $\frac{a}{h_f}$ of up to 0.71 might be generated, this being an accepted maximum unbroken wave height.

Bores formed for runs 28, 30, 31, 33 and 42-45. For these runs values of $\frac{l}{h_f}$, $\frac{\rho_s d}{\rho_f h_f}$, and $\frac{H+d'}{h_f}$ were all large. The bores subsided rapidly over the first 30 water depths along the channel, then gained up to 8% in height as they transformed from broken waves into solitary waves at distances about 60 water depths from the block. The solitary waves so formed had values of $\frac{a}{h_f}$ around 0.50, certainly less than the 0.63 normal maximum unbroken wave heights. These cases illustrated a bistability in which for a given wave height in a range 0.5 to 0.6, a wave could exist in either a broken or unbroken form.

The existence of a non-zero value of $\frac{\delta}{h_f}$ was equivalent to a reduction in the effective length of the falling block. The gap between the end of the channel and the back of the block allowed another path for water to escape from under the block. This reduced the amount of water available to form the hump of water in front of the block. It also reduced the maximum pressures under the block (see Fig. 7.4), nevertheless these pressures could still be very large. For runs 26-33 and 40-47, where values of $\frac{l}{h_f}$, $\frac{\rho_s d}{\rho_f h_f}$, and $\frac{H+d'}{h_f}$ were often all large, water escaping behind

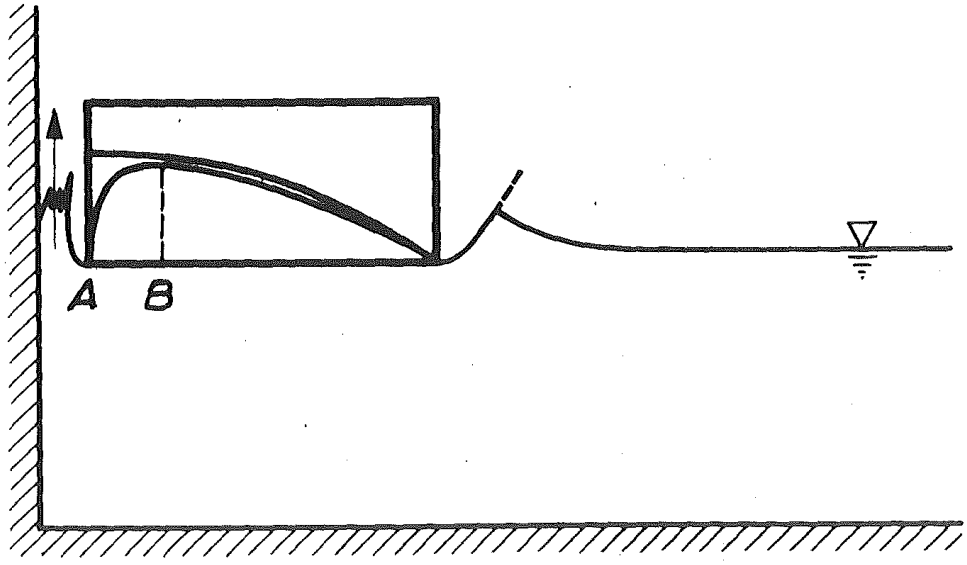

Figure 7.4

Effect of finite $\frac{\delta}{h_f}$ on the pressure distribution under the block as it strikes the water surface.

the falling block regularly reached the laboratory roof above the dropping structure, implying pressure heads of 10 to 15 water depths occurring under the falling block.

When $\frac{\delta}{h_f}$ is zero a stagnation point forms at the rear of the block (point A in Fig. 7.4), and the pressure distribution along the base of the block is thought to be parabolic, as shown. For small $\frac{\delta}{h_f}$ the stagnation point is close to the back of the block as it strikes the water surface. A high pressure gradient near the point A

exists and the vertical water velocity through the gap is high. As $\frac{\delta}{h_f}$ becomes larger the stagnation point under the block as it strikes the water will slowly move away from the rear of the block.

This movement also occurs as the block falls through the water towards the channel floor. Figure 7.5 shows the expected form of the pressure distribution along the underside of the block as it approaches the channel floor.

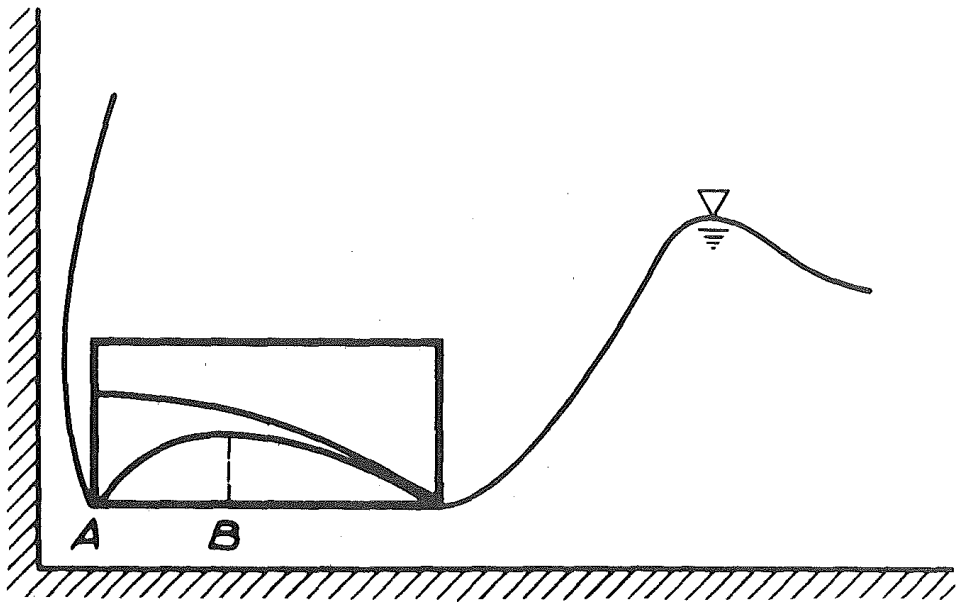

Figure 7.5
Pressure distribution under the block as it nears the channel floor.

The pressure drop in the vicinity of point A is smaller compared with the maximum pressure of B. During this stage the position of the stagnation point is determined

by the parameters $\frac{\delta}{h_f}$ and $\frac{\delta}{y}$ where y is the instantaneous distance between the underside of the falling block and the channel floor. If $\frac{\delta}{h_f}$ is finite then the value of $\frac{\delta}{y}$ increases continually as the block falls; when the block rests on the channel floor $y = 0$ and $\frac{\delta}{y}$ is infinite. Thus as the block falls through the water, the stagnation point B is expected to always approach the centre of the block unless $\frac{\delta}{h_f} = 0$ when the stagnation point remains at the rear end of the block. The position of point B, expressed as a fraction of a block length from the rear end of the block, is thought to be a function of $\frac{\delta}{h_f}$ and $\frac{\delta}{y}$ alone. Parameters like $\frac{\rho_s d}{\rho_f h_f}$, $\frac{l}{h_f}$, and $\frac{H + d'}{h_f}$ affect the maximum water velocities and accelerations but not the position of the stagnation point.

Figure 7.6 shows the manner in which the stagnation point B is thought to move as a block falls through the water. For very small $\frac{\delta}{h_f}$ and very large $\frac{\delta}{h_f}$ the point B does not move appreciably for most, if not all of the block fall, whereas for intermediate values of $\frac{\delta}{h_f}$ (probably between about 0.2 and 1.0) the position of the stagnation point B changes rapidly as the block falls through the region of water near the original water surface.

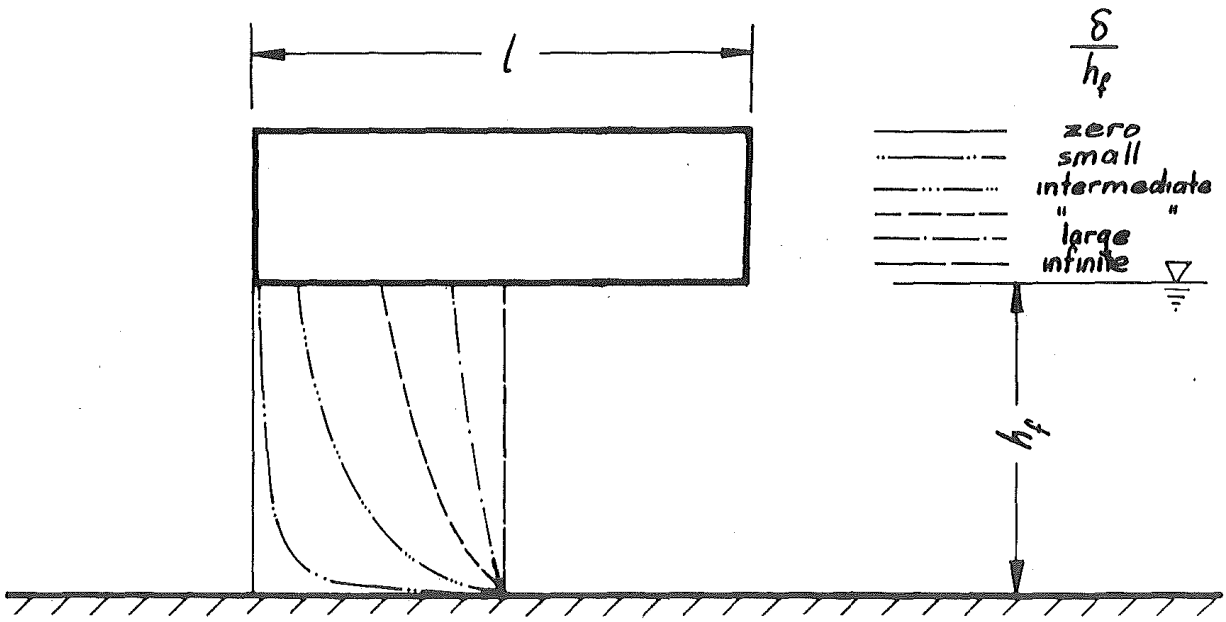

Figure 7.6

Movement of stagnation point B as the block falls through the water

The position of the stagnation point is of importance in two respects:

(a) It controls the division of flow under the block; water flows in either direction from the position of the stagnation point.

(b) It controls the pressure distribution along the underside of the block.

The sum of all the pressures is the force which, acting against the force of gravity on the block, decelerates it to zero velocity as it touches the channel floor.

As Figure 7.4 shows, even a small value of $\frac{\delta}{h_f}$ causes an appreciable decrease in the decelerating force applied to the block. Figure 7.5 shows that the decelerating force is further reduced as the block approaches the channel floor.

Because the retarding force is lessened considerably by the presence of a small $\frac{\delta}{h_f}$, the block falls faster towards the channel floor and is slowed down in a shorter distance just above the floor than for a block falling with $\frac{\delta}{h_f} = 0$. Thus although less water is pushed out under the front of the block, it is pushed out faster and the reduction in first wave height $\frac{a}{h_f}$ is not as marked as would be expected at first glance.

In all the experimental tests a lower limit $\frac{d'}{h_f}$, was set on $\frac{y}{h_f}$, this determining the distance between the fallen block and the channel floor.

Figure 7.7(a) shows how $\frac{\delta}{h_f}$ and $\frac{d'}{h_f}$ affected the first wave height $\frac{a}{h_f}$ at various points along the channel. One important point to note from Figure 7.7(a) is that the manner in which $\frac{\delta}{h_f}$ and $\frac{d'}{h_f}$ affect $\frac{a}{h_f}$ is independent of the distance from the block that $\frac{a}{h_f}$ is measured at; this point is further discussed in Section C of this chapter. Because of this a standard $f(\frac{\delta}{h_f}, \frac{d'}{h_f})$ family of curves can be drawn, as in Figure 7.7(b). The graph is derived from results of Runs 48-87, only some of which are shown in Figure

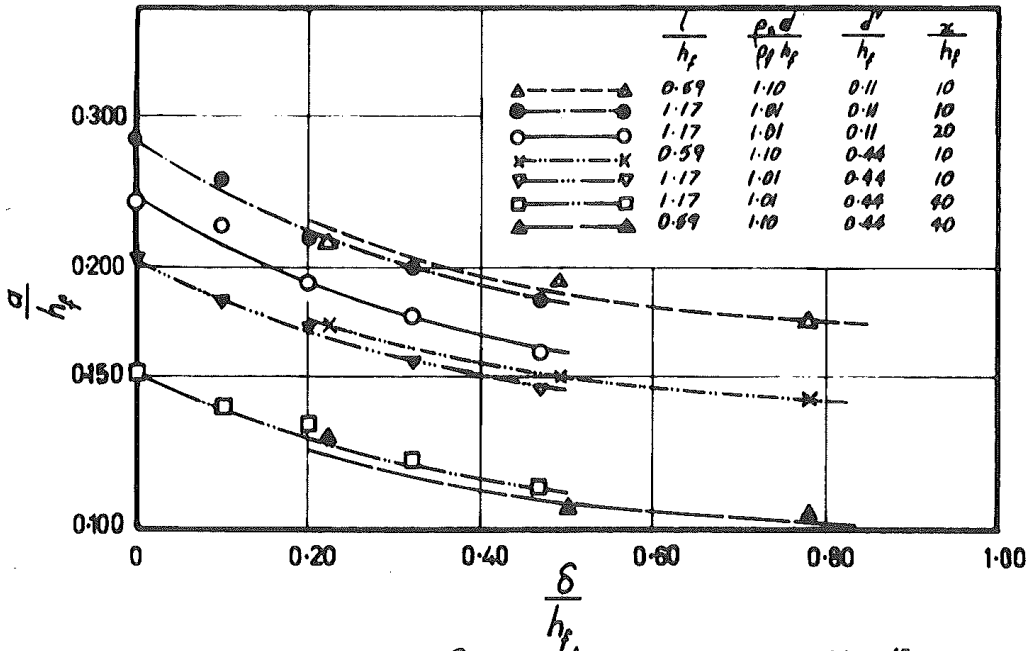

Fig. 7.7(a) $\frac{a}{h_f}$ versus $\frac{\delta}{h_f}$ for $\frac{l}{h_f} = 1.17$ and $\frac{H+d'}{h_f} = 1.34$

$\frac{2a}{h_f}$ versus $\frac{\delta}{h_f}$ for $\frac{l}{h_f} = 0.59$ and $\frac{H+d'}{h_f} = 1.34$

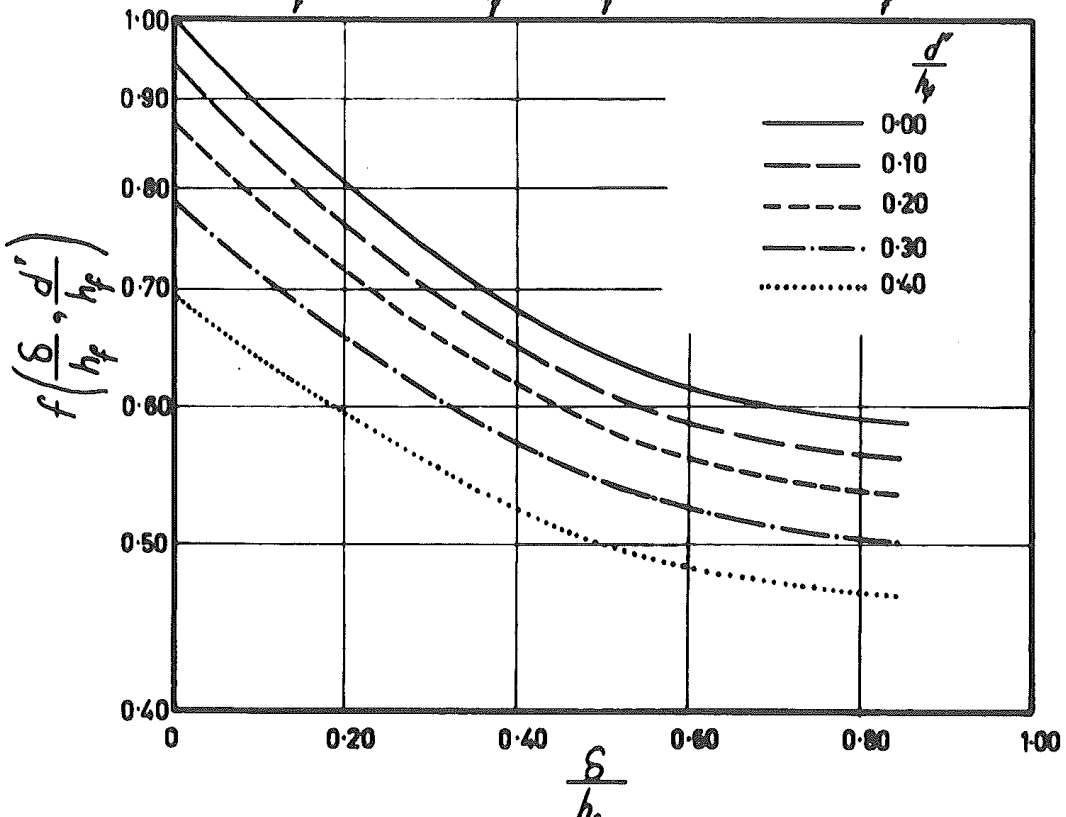

Fig. 7.7(b) Function $f\left(\frac{\delta}{h_f}, \frac{d'}{h_f}\right)$ versus $\frac{\delta}{h_f}$ for varying $\frac{d'}{h_f}$.

7.7(a) for reasons of clarity. Only Runs 84-87 give results which do not follow the trends of the remainder of the results. Reasons for these discrepancies are not known but they are assumed to not detract from the value of Figure 7.7(b).

Figure 7.7(b) shows that $\frac{a}{h_f}$ becomes less dependent on $\frac{\delta}{h_f}$ as $\frac{\delta}{h_f}$ becomes large, i.e. (assuming $\frac{d'}{h_f} = 0$) by the time $\frac{\delta}{h_f}$ has reached 0.8, the first wave height has been reduced to 59% of its maximum value. Further increases in $\frac{\delta}{h_f}$ can cause no more than 9% further reduction in $\frac{a}{h_f}$ since for very large $\frac{\delta}{h_f}$ the effective block length and hence the first wave height are half their values for $\frac{\delta}{h_f} = 0$.

Figure 7.7(b) also shows that as $\frac{d'}{h_f}$ decreases $\frac{a}{h_f}$ increases, although at a reduced rate since the rate of displacement of water from under the block decreases as the block approaches the channel floor. When $\frac{\delta}{h_f} = 0$ the rate of increase in $\frac{a}{h_f}$ as $\frac{d'}{h_f}$ decreases is appreciably larger than when the value of $\frac{\delta}{h_f}$ is in the vicinity of 0.60. This is in line with the reasoning above which suggests that a block falls faster and is decelerated nearer the channel floor when $\frac{\delta}{h_f}$ has an intermediate value than when $\frac{\delta}{h_f} = 0$ or is small.

One effect not visible in Figure 7.7(b) is the gradual diverging of the curves of constant $\frac{d'}{h_f}$ as $\frac{\delta}{h_f}$ becomes large. This is expected as the stagnation point B in Figs. 7.4 and 7.5 approaches the centre of the block and the block behaves

as if its length was halved and $\frac{\delta}{h_f} = 0$. The limited range of $\frac{\delta}{h_f}$ covered probably accounts for this lack of divergence.

Figure 7.7(a) and 7.7(b) are graphs drawn for a constant $\frac{H + d'}{h_f} = 1.34$. Other relationships derived in this study are for $\frac{H + d'}{h_f} = 1.00$, however the errors introduced in this discrepancy are thought to be negligible.

SECTION B. The collapse of the hump both away from the block and back onto the block

As mentioned in Chapter 6, "Results", the hump of water formed just in front of the block such that the front face of the falling block was dry. Once the block had fallen to the limit dictated by $\frac{d'}{h_f}$, whether it be the channel floor or some height above it, the generation of the hump ceased and all ensuing motion was due to the collapse of the hump.

The collapse may be defined as starting when surface velocities, except in the region immediate to the bottom of the falling block, all cease to have components in the direction horizontally away from the block and all cease to have components in the direction vertically away from the channel floor. Thus a hump can start collapsing while the block is still falling, as is almost happening in Photo 6.1,

and can easily be imagined to happen when a block with low $\frac{l}{h_f}$, $\frac{\rho_s d}{\rho_f h_f}$, and $\frac{H+d'}{h_f}$ falls slowly into a channel, with water collapsing back over the block as it falls. In most of the experiments conducted by Weigel (3) the humps formed by falling blocks would have started to collapse before the blocks reached the channel floor.

The sequence of frames, Photos. 6.9 to 6.34, show that the collapse started before Photo 6.16; the rear face of the top of the hump began to flatten before the hump had reached its maximum height. (This coincides roughly with the instant the block comes to rest, Photo 6.15). By Photo 6.18 not only had the hump subsided but also a large part of the water had ceased to move forward. Waves had moved away in either direction, one being the first wave to pass the measuring stations, and the other being the wave which strikes the front face of the block (see Photo 6.20). In the following discussions the latter wave will be referred to as the collapse wave.

The area between the waves in Photo 6.20 is about 3 inches below the still water level. It is this trough which forms the first negative wave. The distance between the first positive wave and the trough of the first negative wave is controlled by the distance the first wave travels before the collapse wave reached the front of the block.

This distance is a function of both the velocity at which water is pushed from under the block, and the volume of water ejected. Thus the distance increases with an increase in $\frac{\rho_s d}{\rho_f h_f}$, $\frac{l}{h_f}$ or $\frac{H+d'}{h_f}$ (assuming $\frac{\delta}{h_f}$ and $\frac{d'}{h_f}$ are constant).

The loss of energy involved in a block falling into a channel is thought to vary according to the values of all the independent parameters $\frac{l}{h_f}$, $\frac{\delta}{h_f}$, $\frac{d'}{h_f}$, $\frac{H+d'}{h_f}$, $\frac{d+d'}{h_f}$, and $\frac{\rho_s d}{\rho_f h_f}$. Only a small energy loss occurs when the block strikes the water; the amount, being dependent on the violence with which the block strikes the water surface, is zero for $\frac{H+d'}{h_f}$ equal to or less than unity, and increases as $\frac{H+d'}{h_f}$ increases. As the block nears the channel floor, the kinetic energy of the water being ejected from under the block is not thought to be recoverable and is lost in turbulence.

When a block with large $\frac{l}{h_f}$, $\frac{\rho_s d}{\rho_f h_f}$, and $\frac{H+d'}{h_f}$ falls into a channel, approximately half the hump created is transformed into the first wave, the other half transforming into the collapse wave. If the energy in the hump is assumed to be distributed evenly throughout the hump (a very rough approximation), then when the hump collapses the energy contained in the hump will be distributed fairly evenly between the first wave and the collapse wave. Thus the energy in the

first wave is less than half the energy transferred to the water by the block. Also, because the collapse wave dissipates a large part of its energy when it strikes the block (viz. Photo 6.20) the energy in the following wavetrain is only a small fraction of the initial water energy.

For blocks with small $\frac{H+d'}{h_f}$, $\frac{l}{h_f}$, and $\frac{\rho_s d}{\rho_f h_f}$ the hump will form close to the block (viz. Photo 6.1) and may not even separate from the block. In these cases the collapse wave would not violently dissipate energy, and a greater percentage of its energy would be transferred into the wave train. The energy of the first wave would not increase significantly because the kinetic energy of water ejected from under the block would not be recovered.

In all cases where the falling block possessed value of $\frac{l}{h_f}$, $\frac{\rho_s d}{\rho_f h_f}$, and $\frac{H+d'}{h_f}$ which were not small, the water hump collapse was such that the first wave had travelled several water depths along the channel before the collapse wave struck the block. Only at this late stage did the ratio $\frac{d+d'}{h_f}$ start to influence motion.

In all experiments, the value of $\frac{d+d'}{h_f}$ was of the same order as $\frac{l}{h_f}$, but was never more than marginally greater than unity. Two interesting lines of research were not pursued. These were the investigation of the properties of waves generated by blocks with very large and very small values of $\frac{d+d'}{h_f}$.

A small value could be achieved by using plate steel for a block. In falling, the plate would initially displace the same amount of water as any block with the same value of $\frac{\rho_s d}{\rho_f h_f}$. However, when the water hump collapsed onto the plate a substantial negative wave would probably form due to the onrush of a large area of water onto the plate.

Weigel (3) did drop a lead plate 0.19 inch thick and 6 inches long into a channel with water depths of 0.36, 0.24, and 0.14 ft. The wave heights measured in these tests did not correlate at all well with results from this study. However, a large first trough, roughly equal in amplitude to the first wave, was generated.

The reasons for the lack of correlation between tests are not understood. First wave heights generated by the falling lead plate were less than one-third the amplitude expected from the results of this study. One factor which would contribute to the difference is that the lead plate mentioned above was dropped from a submerged position such that the top of the plate was level with the water surface. The small fall height $\frac{H+d'}{h_f}$ coupled with relatively small $\frac{l}{h_f}$ and $\frac{\rho_s d}{\rho_f h_f}$ may have caused such a low rate of descent of the plate that the hump collapsed onto the top of the plate as it descended. Thus only a small volume (per unit width) of water would be displaced at any time and a small first wave height would result.

The effect of a large value of $\frac{d+d'}{h_f}$ would be to decrease the area into which the hump could collapse (and slightly increase the amount of water ejected upwards as the collapse wave strikes the block). A smaller negative wave would be expected, with the possibility that the first positive wave would be nearly solitary in form. A wave of this sort was noted by Weigel ((3), page 766).

Although the parameter $\frac{d+d'}{h_f}$ is thought to significantly affect the height of the first negative wave, which in turn is thought to influence the subsidence of the first positive wave, the first wave had usually travelled several water depths before the collapse wave struck the block and subsidence over the first ten water depths for the first wave was assumed to be negligible. The first wave height at distance $\frac{x}{h_f} = 10$ was assumed to be the function -

$$\frac{a}{h_f} = f\left(\frac{l}{h_f}, \frac{\rho_s d}{\rho_f h_f}, \frac{H+d'}{h_f}, \frac{\delta}{h_f}, \frac{d'}{h_f}\right)$$

for $x = 10h_f$

The above assumption was borne out by the experimental data.

SECTION C. The subsidence of the wave as it travels along the channel

The subsidence of the first wave was assumed to be due entirely to its asymmetry since energy losses due to viscous effects have been assumed to be negligible (Chapter 5). In nearly all cases the subsidence was found to be expressible in terms of an equation of the form

$$\frac{a}{h_f} = \left(\frac{x}{h_f}\right)^{-m} f\left(\frac{l}{h_f}, \frac{\rho_s d}{\rho_f h_f}, \frac{H+d'}{h_f}, \frac{\delta}{h_f}, \frac{d'}{h_f}, \frac{d+d'}{h_f}\right)$$

where m is a constant.

Originally m was assumed to be dependent on the wave properties $\frac{a}{h_f}$, $\frac{a'}{h_f}$, and $\frac{\lambda}{h_f}$ where:

$\frac{a'}{h_f}$ = first trough depth : water depth ratio,

$\frac{\lambda}{h_f}$ = distance between first crest and first trough : water depth ratio.

The terms $\frac{a'}{h_f}$ and $\frac{\lambda}{h_f}$ were thought to give a measure of the asymmetry of the first wave. However, the subsidence was found to be roughly independent of $\frac{\lambda}{h_f}$ and dependent on $\frac{a}{h_f}$ and $\frac{a'}{h_f}$ (see Figs. 7.8 and 7.9).

Any study of subsidence along these lines involves an experimental solution of the first trough depth $\frac{a'}{h_f}$ in terms of all the relevant parameters, however preliminary studies of

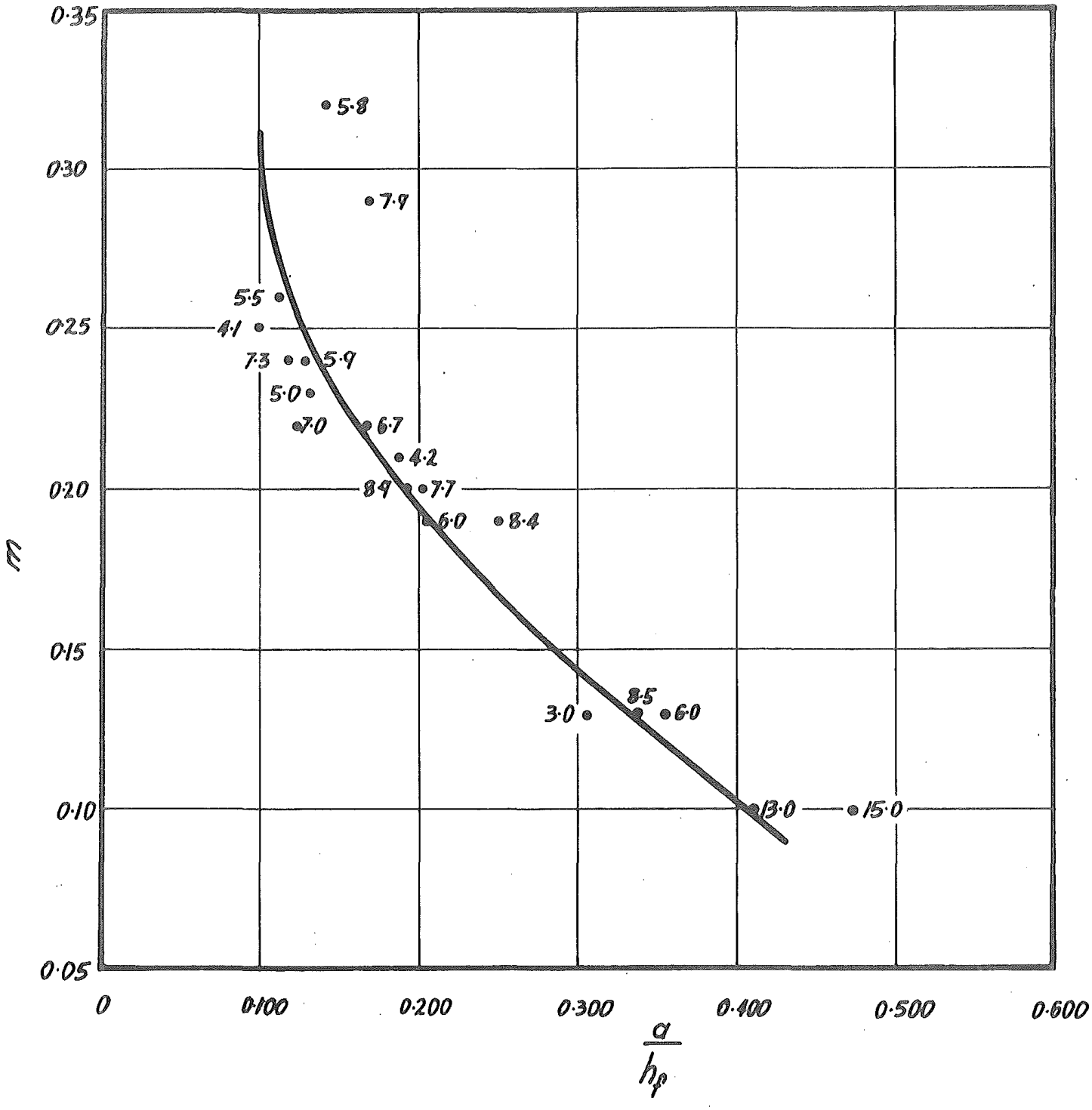

Fig. 7.8. Graph of m versus $\frac{a}{h_f}$ for varying $\frac{\lambda}{h_f}$

$$0.90 < \frac{a'}{h_f} < 0.100$$

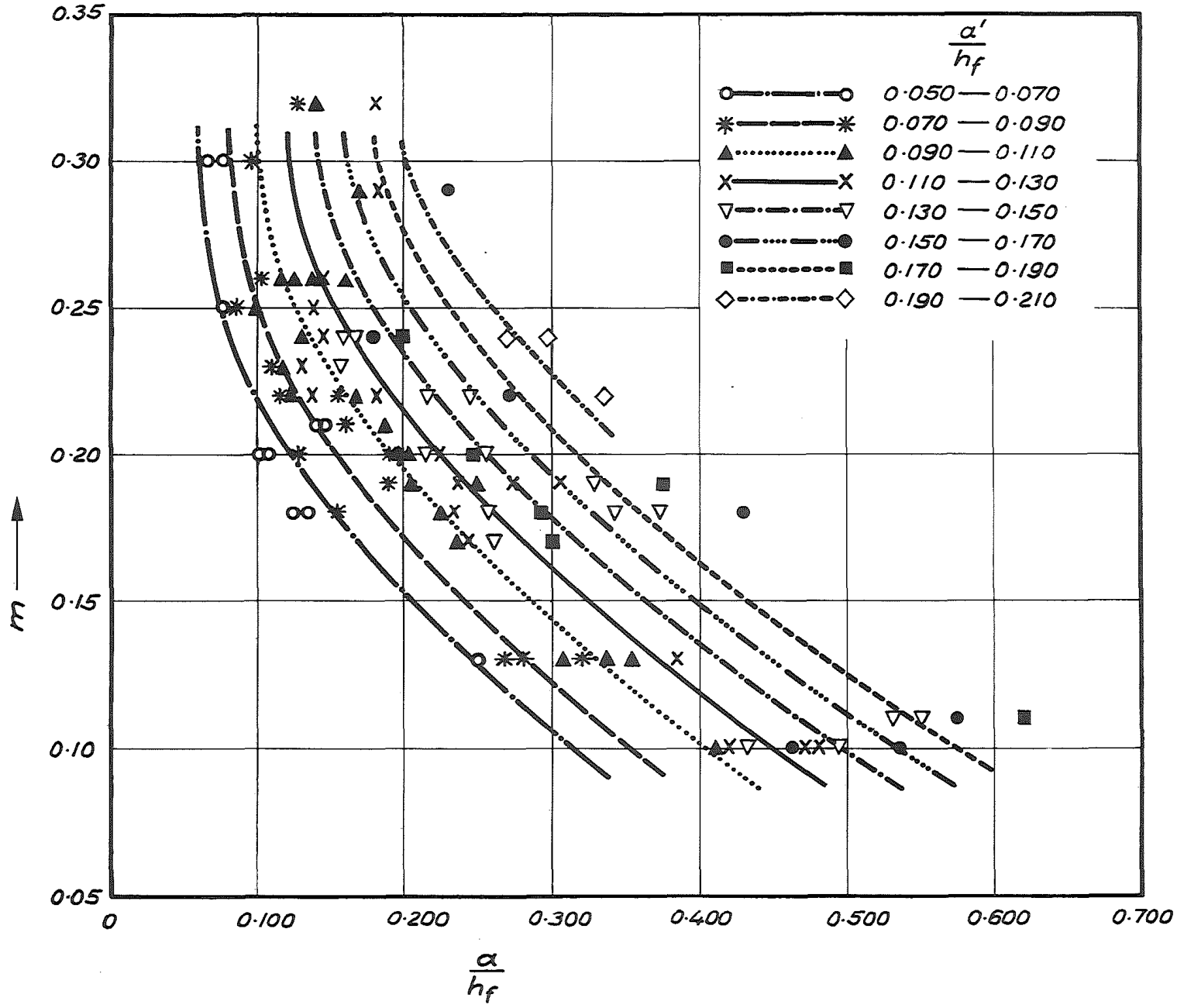

Fig. 7.9. Graph of m versus $\frac{a}{h_f}$ for varying $\frac{a'}{h_f}$

$\frac{a'}{h_f}$ showed that the various parameters which affected $\frac{a}{h_f}$ in the manner described in Sections A and B affected $\frac{a'}{h_f}$ in obscure ways. The value of $\frac{a'}{h_f}$ did depend on $\frac{H+d'}{h_f}$, but not in a regular manner; it did not seem to depend significantly on $\frac{\rho_s d}{\rho_f h_f}$ of $\frac{1}{h_f}$. Thus a search began to determine the subsidence in terms of the parameters used to describe the first wave height, namely:

$$\frac{1}{h_f}, \frac{\rho_s d}{\rho_f h_f}, \frac{H+d'}{h_f}, \frac{d'}{h_f}, \frac{\delta}{h_f}, \text{ and } \frac{d+d'}{h_f}.$$

The total fall height $\frac{H+d'}{h_f}$ affected $\frac{a}{h_f}$ in a way which was dependent to a small extent on the value of $\frac{x}{h_f}$. In Section A it is stated that

$$\frac{a}{h_f} = \frac{1}{h_f}\left(\frac{\rho_s d}{\rho_f h_f}\right)^{0.4}\left(\frac{H+d'}{h_f}\right)^{n} f\left(\frac{\delta}{h_f}, \frac{d'}{h_f}, \frac{d+d'}{h_f}\right)$$

for $x = 10h_f$

where n was a function of $\frac{1}{h_f}$ and $\frac{\rho_s d}{\rho_f h_f}$. The accuracy of measurement of the value of n was poor since measurement of $\frac{a}{h_f}$ were liable to be in error by up to 10%. Thus attempts to measure variations in the value of n are liable to be very inaccurate. An examination of Figure 7.10 shows however that n increases roughly 10% over 40 water depths in most cases. Hence the value of n can be written as

$$n = n_{10} + \frac{x}{400 h_f}$$

where n_{10} denotes the value of n at a distance $x = 10h_f$ from the block.

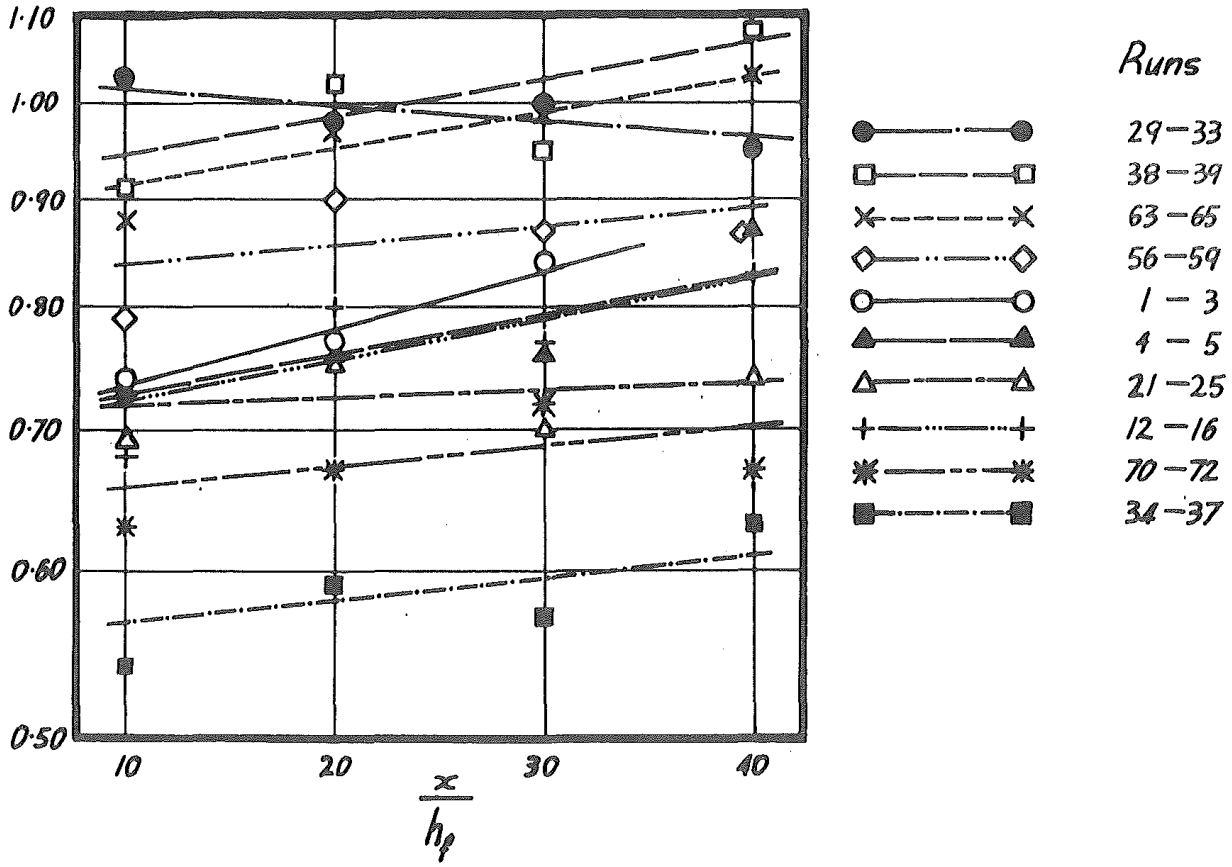

Figure 7.10

Graph of n versus $\frac{x}{h_f}$

The most notable result of the study of subsidence was that it was ostensibly independent of the parameters $\frac{l}{h_f}$, $\frac{\delta}{h_f}$, $\frac{d'}{h_f}$, and $\frac{d+d'}{h_f}$. These parameters describe all the dimensions of the block relative to the water depth in the channel. That none of them markedly affected the subsidence is a quite unexpected result.

Figure 7.11 shows how the subsidence of the first wave was independent of $\frac{l}{h_f}$ for varying $\frac{\delta}{h_f}$ and $\frac{d'}{h_f}$ but for constant $\frac{\rho_s d}{\rho_f h_f}$.

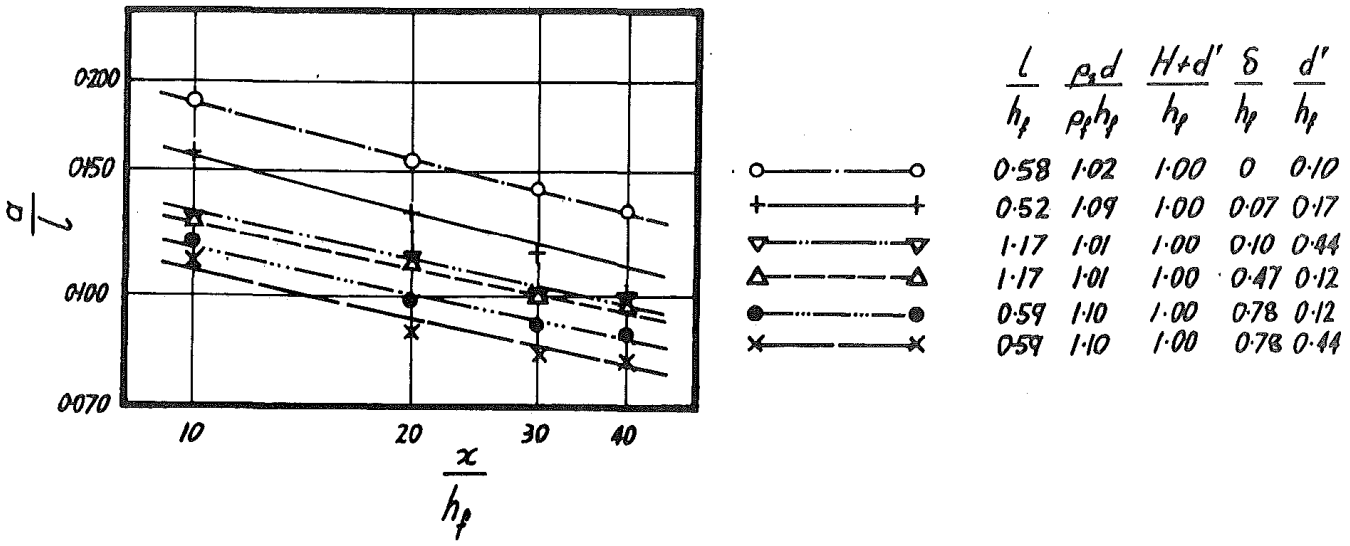

Figure 7.11

Effect on subsidence of varying $\frac{l}{h_f}$ for various $\frac{\delta}{h_f}$, $\frac{d'}{h_f}$, but for constant $\frac{\rho_s d}{\rho_f h_f}$.

Figure 7.7(a) above shows how the effects of $\frac{\delta}{h_f}$ and $\frac{d'}{h_f}$ on $\frac{a}{h_f}$ do not change with distance from the block.

Although the parameter $\frac{d+d'}{h_f}$ was not thought to influence $\frac{a}{h_f}$ at positions close to the block, it was expected to significantly affect the first wave height at large distances from the block. But over the ranges of parameters tested its effects on subsidence could not be found and was for all practical purposes assumed to be

negligible. The implications of this experimental observation are hard to justify even on qualitative grounds. The ratio $\frac{d+d'}{h_f}$ is thought to influence the first trough height (visualise the different effects of a thin plate and a very high block falling into a channel, Section B above). The first trough height does affect the subsidence of the first wave (Fig. 7.9 above) thus the lack of influence of $\frac{d+d'}{h_f}$ on subsidence is rather surprising. A possible explanation is that the range over which $\frac{d+d'}{h_f}$ was tested was sufficiently small, i.e. 0.5 to 1.10 that variations occurring in $\frac{a}{h_f}$ were too small to be distinguished from experimental errors.

Subsidence of the first wave was found to be dependent primarily on the mass flux ratio $\frac{\rho_s d}{\rho_f h_f}$. Figures 7.12 and 7.13 show how the subsidence decreases with increasing $\frac{\rho_s d}{\rho_f h_f}$. The implication of this finding is rather ominous for design engineers - namely that as $\frac{\rho_s d}{\rho_f h_f}$ increases, not only does the initial wave height increase, but the subsidence decreases so that a large distance from the region of a rockfall the wave height is very dependent on $\frac{\rho_s d}{\rho_f h_f}$.

A large scatter exists in Figure 7.13 showing that although the subsidence is mainly affected by $\frac{\rho_s d}{\rho_f h_f}$, it is probably affected by other parameters, the extents of which could not be individually determined within the limits of this experimental study. Probably $\frac{d+d'}{h_f}$ and other

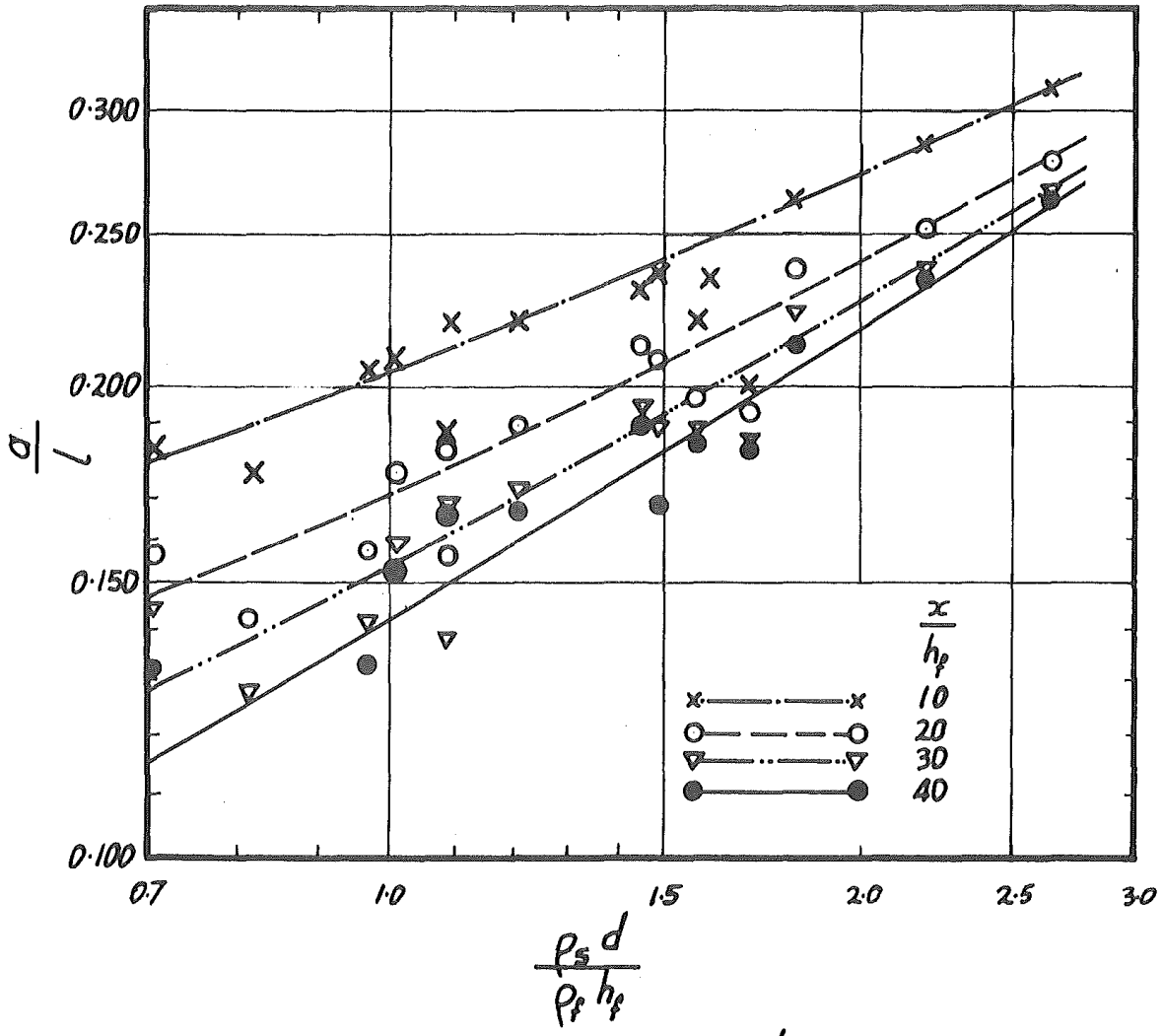

Fig. 7.12. Graph of $\frac{a}{l}$ versus $\frac{\rho_s d}{\rho_f h_f}$ for varying $\frac{x}{h_f}$ with $\frac{\delta}{h_f} = 0$; $\frac{d''}{h_f} = 0$; $\frac{H+d''}{h_f} = 1{\cdot}00$

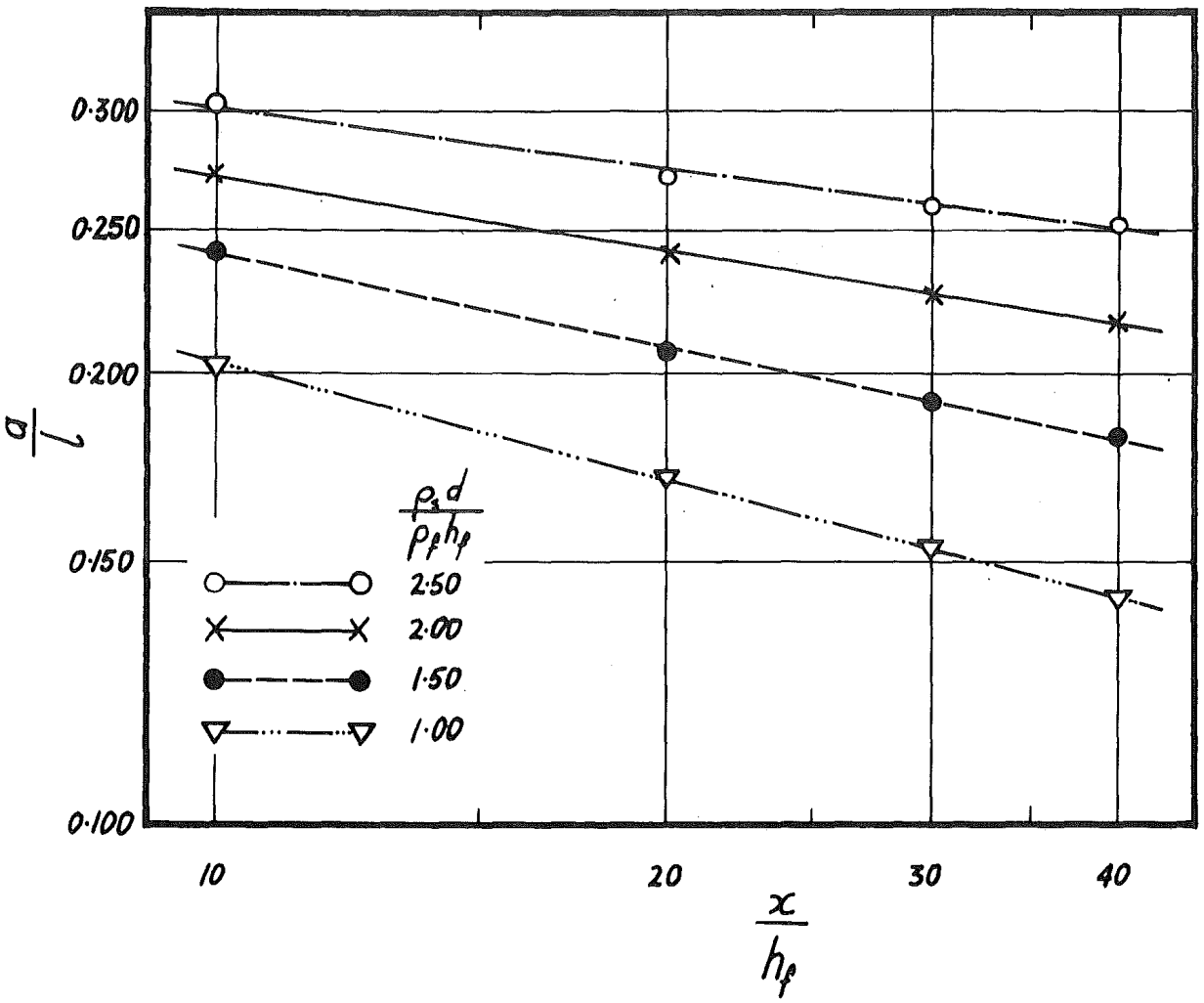

Fig. 7.13. Graph of $\frac{a}{l}$ versus $\frac{x}{h_f}$ for varying $\frac{\rho_s d}{\rho_f h_f}$ with $\frac{\delta}{h_f} = 0$; $\frac{d'}{h_f} = 0$; $\frac{H+d'}{h_f} = 1{\cdot}00$

parameters describing the block dimensions do affect subsidence, but not as much as previously thought.

Notable exceptions to the trends shown in Figures 7.12 and 7.13 are the results for runs 34-37 where $\frac{\rho_s d}{\rho_f h_f} = 0.71$, and runs 26-33 where $\frac{\rho_s d}{\rho_f h_f} = 1.57$ and 1.70. For these three cases the subsidence was much less than anticipated. A possible explanation for this behaviour stems from equation (2) in Section A above (page 47) where there is a suggestion that the motion of the block is controlled by a ratio $\frac{\rho_s d}{\rho_f h_f} / (\frac{l}{h_f})^2$. In the cases above, this ratio is lower than for the remainder of the experiments. A study involving the range of large $(\frac{l}{h_f})^2$ compared with $\frac{\rho_s d}{\rho_f h_f}$ may well elucidate these results and is recommended for future research.

The Wave Train

A cursory study of the characteristics of the extended wave train following the first trough was made.

The length of the wave train was found to be roughly proportional to the distance it had travelled from the block. An estimate of wave height subsidence suggested that it was proportional to $(\frac{x}{h_f})^{-\frac{1}{2}}$. These two observations are in agreement with the conservation of wave energy within the wave train as it travels along the channel.

The length of the wave train was roughly constant for most runs, the exceptions being for runs 26-33 and 40-47 when $\frac{1}{h_f}$, $\frac{\rho_s d}{\rho_f h_f}$, and $\frac{H+d'}{h_f}$ were large. (For these runs the length of the wave train was reduced, the reasons for which are not known). The end of the wave train usually passed the first station (at 16 ft. from the block) at about the same time that the first wave had travelled 50 ft. Allowing for the distance between the first wave and the wave train, the wave train can be seen to extend over about 25 feet at this stage.

There was little evidence of nodal points in the wave group amplitudes but the general form of the group amplitudes could vary substantially. Examples are given in Fig. 7.14.

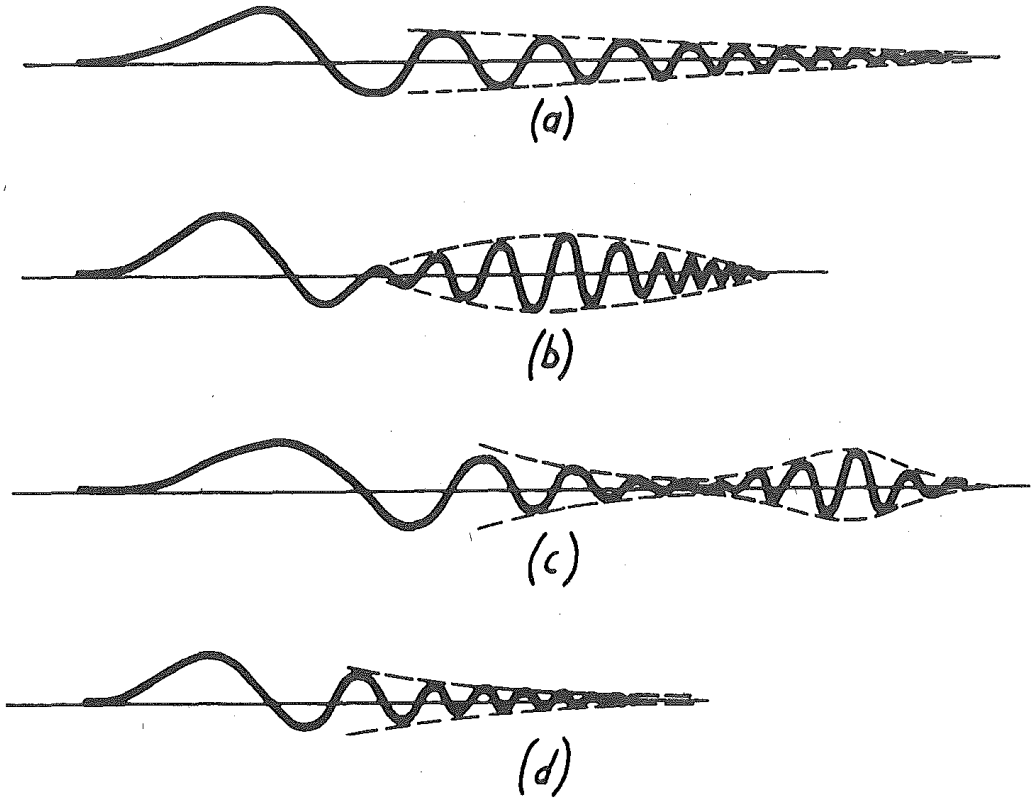

Fig. 7.14 General forms of group amplitudes.

There did not seem to be any pattern in the forms of group amplitude except that example (d) tended to exist predominantly for larger values of $\frac{l}{h_f}$, $\frac{\rho_s d}{\rho_f h_f}$, and $\frac{H+d'}{h_f}$. In these cases the first peak of the wave train was often broken for up to about ten water depths.

The overall shape of the wave train did not vary as it proceeded along the channel. Generally the maximum amplitude measured in the wave train was less than the first wave height but only rarely exceeded 0.20 water depth even at points close to the block.

CHAPTER 8

ERROR SOURCES

The sources of error in each measurement are noted.

Water Depth

A small seche, usually less than 2% water depth peak to peak amplitude, could develop in the channel. The period, depending on water depth, was of the order of half a minute. An average reading could be made of water depth by measuring the depth continuously over a period; the actual water depth at the instant the block fell was taken to be the average value. The floor of the channel was horizontal to within less than $\frac{1}{8}$ inch, and with water depths usually of the order of 16 inches the maximum error due to floor unevenness is about 0.7%. Thus an error of just over 1% could exist in this measurement.

Water Density

The water temperature was always within about two degrees of 60°F. There were very few impurities in it, and its density was taken as 62.4 lb/cu.ft. Any error in its density was considered to be so small as to be negligible.

Block Dimensions

The blocks were very accurately constructed and all

faces could be considered to be at right angles to adjacent faces. The outside dimensions could be measured with negligible error. The width of all blocks was 23¼ inches, i.e. ¾ inch less than the channel width. The effect of this 3% discrepancy is not known. It is presumably small, since in the photo of the block falling into the channel, Fig. 6.13, there seems to be no appreciable amount of water escaping up the gaps between the block and the channel wall. The error involved in assuming the block fits perfectly across the channel is thought to be less than 3%.

Block Density and the Effects of the Dropping Structure Shafts

The block weight could be measured by weighing the submerged block on the large tension spring in the dropping structure. Since the volume of the block could be accurately determined, the weight of water displaced was known. Adding this to the submerged weight derived from the spring extension gave the true weight of the block in air. In this way the block weight was measured in situ - an advantage when the block density was being varied. Errors in weighing the block were reduced by multiple readings of the spring extension, and probably amounted to about 1%.

Calculation of the block density is complicated by the shafts of the dropping structure, which pass through 2¼ inch square holes in the bottom of the blocks. The volume of a

block was calculated from the height and gross base area of the block. Thus the block density, being weight/volume, was in error by about 4% for the 9.5" x 8.3" block and less for the other blocks, this error being a consistent error for each block. A study of Figure 7.12 shows that an error in block density of 4% causes an error of about 2% in first wave height.

The shafts also interfered with the water flow underneath the block by providing a constriction from 24 inches width to about 20 inches width, thus representing an 8% reduction in width. However the mean water velocity between the shafts was roughly one-half the velocity under the front face of the block for small values of $\frac{\delta}{h_f}$, and lessened as $\frac{\delta}{h_f}$ increased. Thus energy losses due to the presence of the shafts were small compared with the energy of water passing under the front face of the block. An estimate of the error in water velocity caused by assuming the shafts did not exist would be about 2%. The error this causes in first wave height is thought to be of the same order.

Distance Between Back of Block and End Wall

Because there was some clearance between the dropping structure shafts and the block, roughly $\frac{1}{8}$ inch, some slight variations in the distance between the back face of the block and the end wall could occur, depending on how the block fell.

The effect of this variation becomes more marked only as $\frac{\delta}{h_f}$ becomes small (viz. Fig. 7.7(b)), but never causes a variation of more than about 1% in first wave height for water depths of about 16 inches.

Distance Between Bottom of Fallen Block and Channel Floor

This distance was measured under water and was liable to an error of up to $\frac{1}{8}$ inch. From Figure 7.7(a) the error in first wave height on water about 16 inches deep was thus possibly 0.5%.

Initial Height of Block

The measurement of the height the block fell through could be made to within about 0.1 inch. When the possible error in measurement of the distance between the bottom of the fallen block and the channel floor is added, a maximum error of about 0.2 inch could occur. However, the initial height of the block was usually greater than 20 inches, implying a maximum error of less than 1% in first wave heights.

Wave Heights

The traces formed on the paper from the oscilloscript were rather broad, reducing reading accuracy. Also, because of the asymmetry of the first wave and first trough, each height had to be measured relative to the still water level. Because a small seche could develop, and because of the hysterysis effect (see Appendix II) in the measuring equipment,

some uncertainty could exist in determining the position of the mean water level on the oscilloscript trace. This uncertainty affected the first trough much more than the first crest, since in some cases the uncertainty represented up to 30% of the first trough height.

The averaging provided by several calibrations and one repeat of every run did help to eliminate these errors. The maximum error in obtaining first wave heights from the traces is thought to be about 5%, this figure increasing for measurements of first trough heights.

The method of calibration involved an important source of inaccuracy. The conduction of current between two parallel rods, one with a voltage applied to it, the other at earth potential, immersed in water at earth potential, is influenced to some extent by the boundaries of the water in which the rods are submerged. In water which was very deep relative to submerged probe length, calibration by raising and lowering the probes is accurate. However, in shallow water a wave passing a probe is thought to vary the conductance in a different manner from varying the submergence of the probe in still water.

The differences involved have not been estimated quantitatively in this study, however, Weigel ((3), page 769) mentions that for probes which presumably are calibrated by

this method, the probable maximum error is 5%. Thus the total error in wave height measurement could reach 10%.

Time Measurement

The speed of paper travelling through the oscilloscript was found to be 5 cm/sec to within about 1%. Measurements of times at which crests or troughs passed the probes could be made to within 0.05 sec., i.e. to the nearest 0.1 sec.

CHAPTER 9

CONCLUSIONS

Within its limitations this study showed that of the waves produced by a block falling into shallow water, the first, or leading wave was positive and usually of larger amplitude than any other wave generated. Its speed was very nearly equal to the speed of a solitary wave of the same height, and was appreciably faster than all the other waves generated. Because of these properties the first wave was considered to be the most important cause of wave damage resulting from a large rockfall into a reservoir.

An experimental solution to the rockfall problem in a two-dimensional channel is proposed. It is acknowledged to have inadequacies but, within the ranges covered by the study is believed to be more accurate and more rational than other published experimental works. All parameters used were chosen to represent quantities which could be readily estimated at a potential rockfall site.

The results are discussed in Chapter 7 and the conclusions reached in the discussion are given below.

(i) The first wave height was found to be nearly linearly proportional to the block length.

(ii) The existence of a gap between the rear of the block and the end of the channel altered the flow pattern under the block and reduced the first wave height. As the gap size became large relative to the water depth, the first wave height reduced towards one half of the zero-gap first wave height.

(iii) A term called the mass flux ratio was formed which related the block density and height to the water density and depth. The first wave height increased as the mass flux ratio increased.

(iv) The height above the channel floor from which a block fell affected the first wave height, the manner being dependent on the values of mass flux ratio and block length/water depth ratio. As the height increased, larger first waves were formed.

(v) The height to which the block fell above the channel floor affected the first wave height in a manner dependent on the size of the gap between the rear of the block and the end of the channel. An increase in the height to which the block fell caused a decrease in first wave height.

(vi) The distance between the top of the fallen block and the channel floor was thought to affect the subsidence of the first wave, however, over the range tested in this study, its effect was found to be negligible. Only a small range

was tested and a more comprehensive investigation into this aspect of subsidence is recommended for future study.

(vii) The subsidence of the first wave as it proceeded along the channel was found to be ostensibly independent of all the block dimensions. The only parameter which influenced the subsidence to any appreciable extent was the mass flux ratio.

(viii) A study of first wave heights generated by falling blocks with small values of mass flux ratios compared with the squares of the block length : water depth ratios may well elucidate some irregularities found in this study. For these blocks the heights of the first waves generated did not seem to be linearly proportional to the block length and the subsidences were less than anticipated.

Appendix I

Photographs and Drawings of the Experimental Set-up

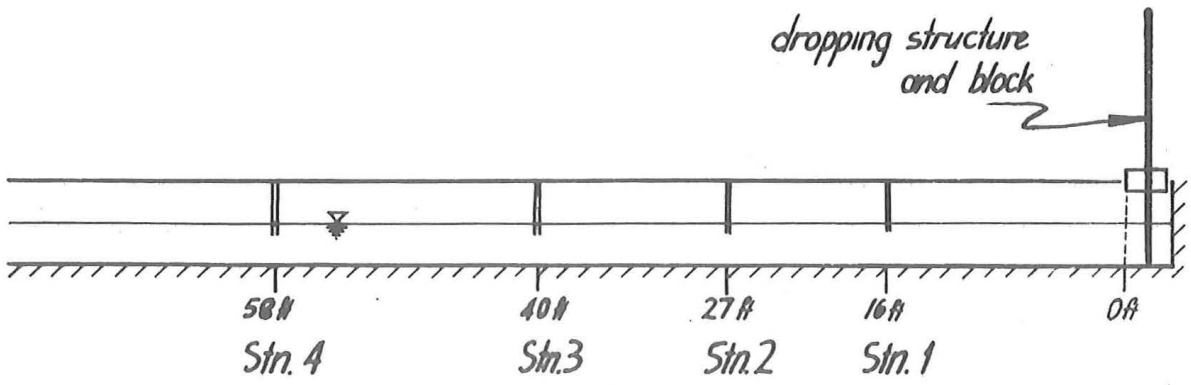

Fig. AI.1. Schematic Diagram of Experimental Setup (not to scale)

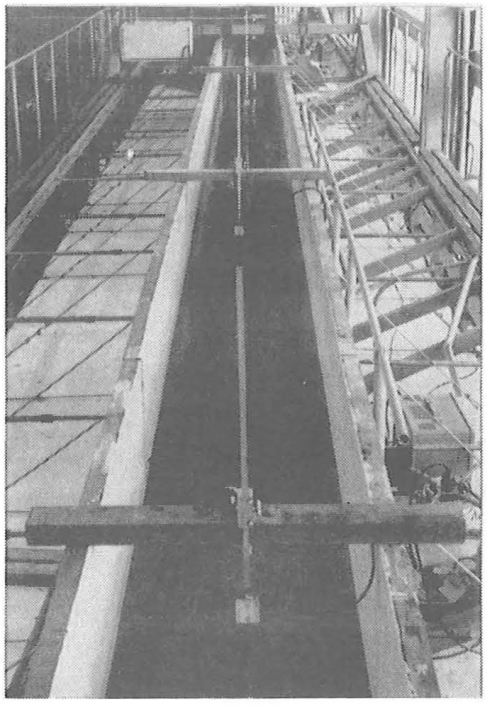

Fig. AI.2. View of channel looking away from the dropping structure. Measuring Stations 1, 2, and 3 can be seen.

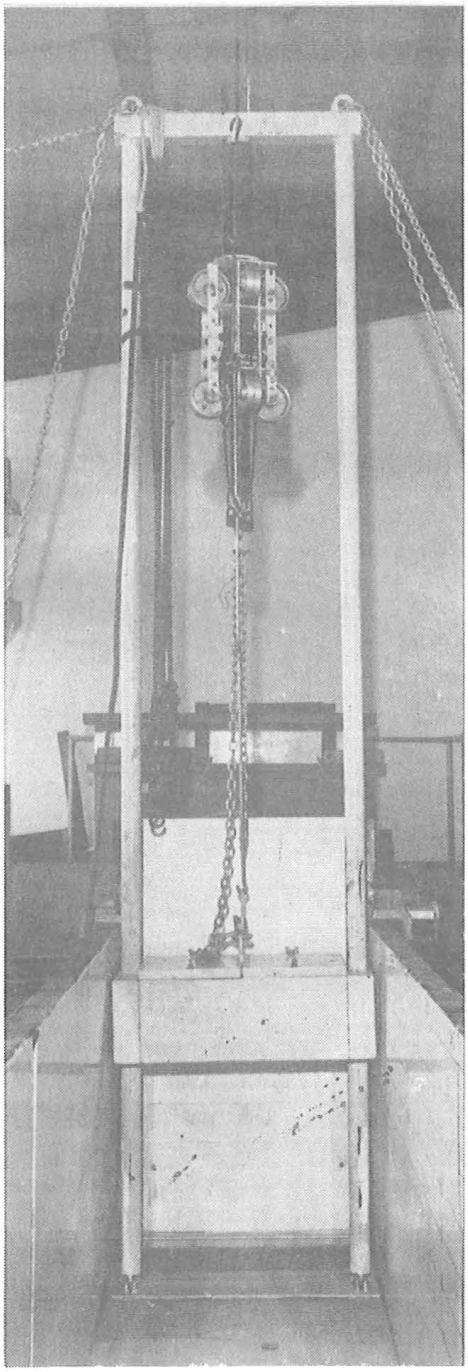

Fig. AI. 3. View of dropping structure, block, and backboard. The top of the dropping structure is 9 ft above the channel floor. Note the non-return cursor above the dropping structure; it measures the spring extension via a rod connected to the distribution bar below the brake.

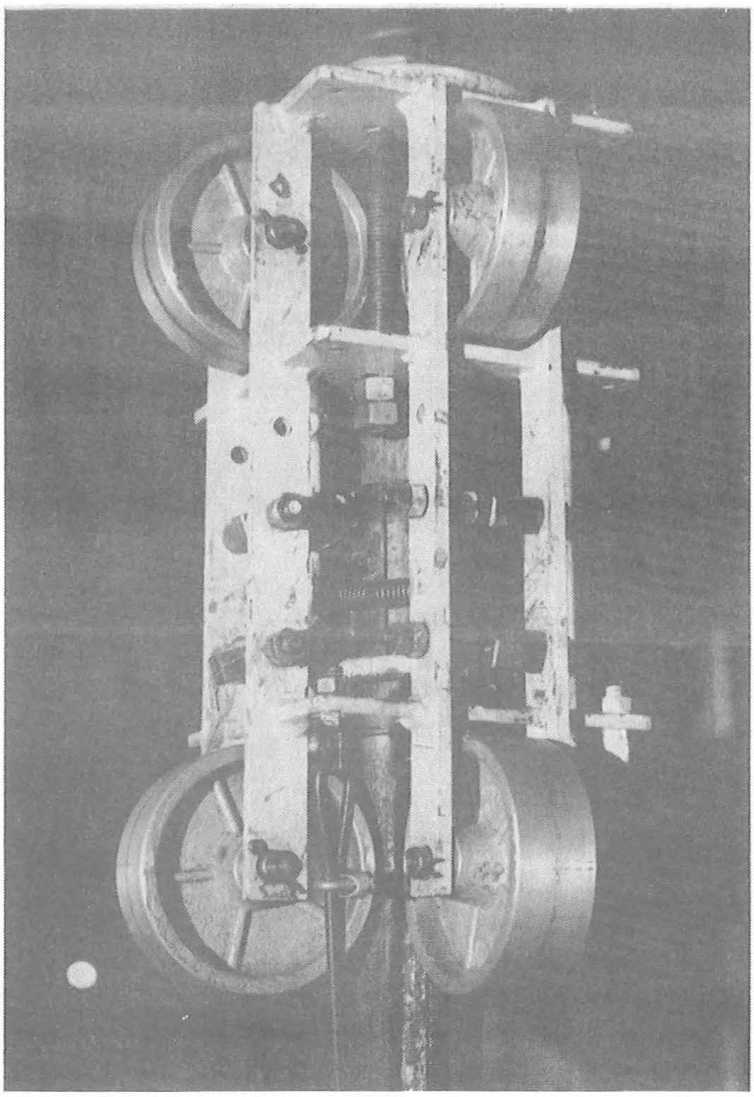

Fig. AI.4. View of spring-brake mechanism, showing the spring-brake connection, the circular spring holding the brake pads onto the shaft, and the links leading from the brake to the distribution bar and thence to the chain and block.

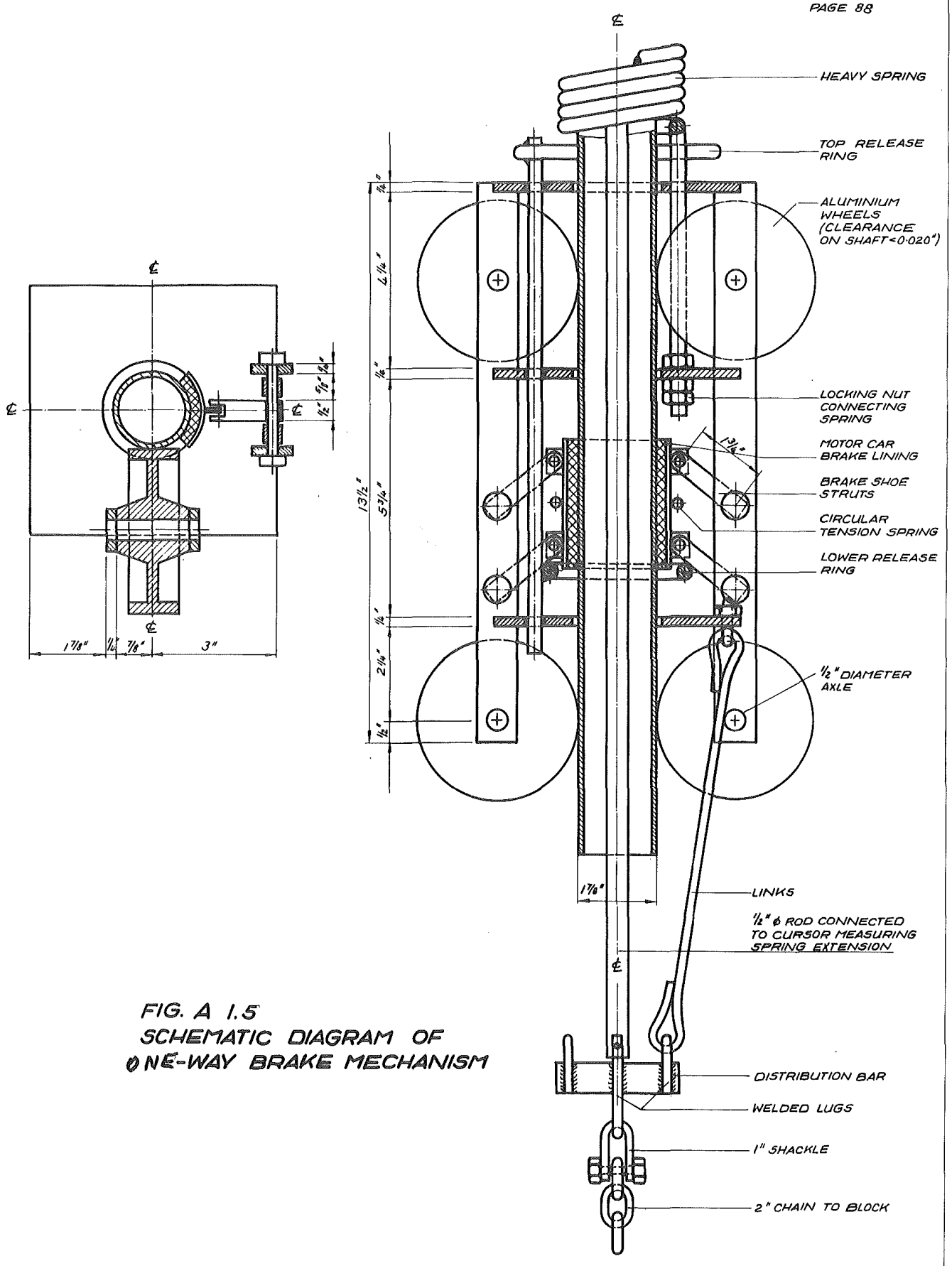

FIG. A 1.5
SCHEMATIC DIAGRAM OF
ONE-WAY BRAKE MECHANISM

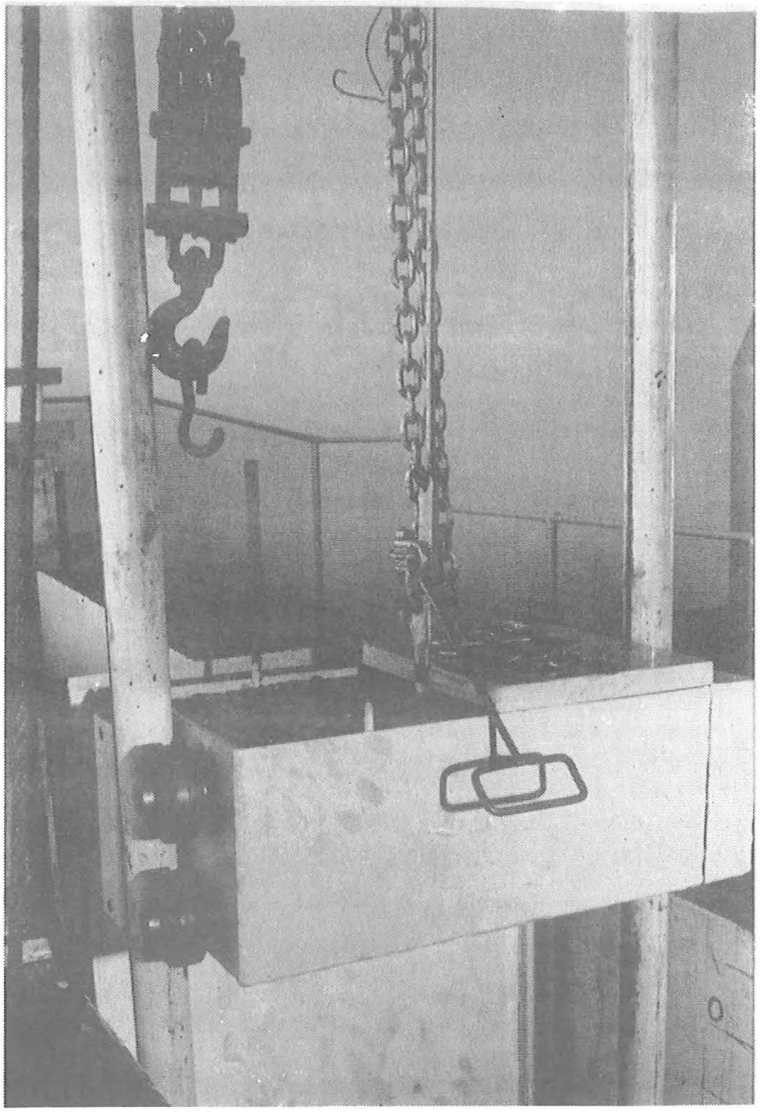

Fig. AI.6. View showing the hollow construction of the block. It is filled with gravel and water. The block weight is held by a shackle which fits in a notch in the metal strip on the connecting links. The block falls when the strip is pulled from the shackle. Wheels on the block reduce friction between the guiding shafts of the dropping structure and the falling block.

APPENDIX 2

EXPERIMENTAL TECHNIQUE

Considerable time was spent developing equipment to give satisfactory performance.

The spring in the dropping structure was accurately calibrated before being mounted. Its stiffness was very close to 224 lb/in for extensions up to 7".

The non-return brake provided some development problems. Initially rubber brake pads bearing on the central shaft were tried, without success, since the rubber did not bond satisfactorily to the brake shoes. When the central shaft was wet the brake failed to hold at all, and even when completely dry it slowly crept upward at rates up to about 0.05 in/sec. These failings meant that appreciable errors in measurements of the block's total fall height and the spring extension could occur. The use of motorcar brake shoe material on the shoes overcame this problem to a large extent. Appropriate adjustments to the lengths of the struts supporting the brake shoes were required to allow for the smaller coefficient of friction between the shoes and the central shaft. Even this brake material was of limited use if the brake or shaft was severely splashed.

Only one strut per brake shoe was thought to be required, however, with this system the brake often failed due to dislocation of one or more of the four brake shoes. This caused the non-return brake to be unsatisfactory in operation. Attaching another strut to each shoe was sufficient to rectify the situation. Not only did the additional struts provide the shoes with a parallel arm action, but they reduced the loads induced by the shoes on each strut.

Originally, proprietary hard rubber wheels were used on the brake carrier to reduce friction losses as the brake was pulled down by the falling block. However, these proved sufficiently elastic for the shoes to force the struts to invert themselves when for some reason the shoes took up loads unevenly. The use of aluminium wheels, with very little clearance on the central shaft, overcame this problem.

The mechanical losses in the dropping structure were estimated by letting blocks fall in air alone. The difference between the potential energy loss of the fallen block and the energy absorbed in the large spring must have been the energy dissipated in losses. Nearly all the losses occurred in the spring non-return brake system, very little being caused by friction between the dropping structure shafts and the falling block (see Appendix 1 for details). Because of this, the block was assumed to fall unimpeded by the dropping structure until the spring-brake system started retarding the block. The losses were included in the impulse the block received

from the spring-brake system.

Frequent calibration of the electronic wave-measuring equipment was found to be necessary. Small voltage drifts occurred throughout a day's testing, and especially over the first few runs of the day. These could be satisfactorily measured after allowing the equipment to warm up for 90 min. before the first calibration and commencement of testing. Calibrations were then made at half-hour intervals initially, then hour to hour and a half intervals as the day progressed.

Description of a Run

Each run was repeated once to reduce errors. At the beginning of each run the oscilloscript was started and the block was released to fall into the channel. After the wave generated by the block had passed all four measuring probes, the oscilloscript was stopped. Measurements of spring extension, block fall height, and distance between the fallen block and the channel floor were made. The non-return brake was slowly released, so that the spring used its stored energy in raising the block and heating the brake shoes.

If any alteration in the height from which the block fell was required, the coupling rods were changed and the block was raised from the water and connected to them. If the height to which the block fell was to be varied, the chain

length was altered at this stage while all the block's weight was taken by the coupling rods. The distance between the back of the block and the end of the channel, and the block density, were also altered as required.

The non-return cursor on the scale above the spring was returned and read to give the zero spring extension reading for the next run. A delay of about 8 - 10 minutes was required before the next run to allow the water surface to become level.

Analysis of Results

The analysis of results involved the formation of several dimensionless parameters of:

(i) the independent variables, i.e. those describing dimensions associated with the block;

(ii) the dependent variables, i.e. those dimensions describing wave properties and block impulse.

The independent variables could all be calculated easily. The water depth, block dimensions, total block fall height, height of fallen block above the channel floor, and distance between the back of the block and the end of the channel, could all be directly measured. The density

of the block could be calculated from measurements of block weight and block dimensions. From the above, all the parameters referred to in (i) above could be formed, i.e.

$$\frac{l}{h_f}\ ,\ \frac{\rho_s d}{\rho_f h_f}\ ,\ \frac{H+d'}{h_f}\ ,\ \frac{\delta}{h_f}\ ,\ \frac{d'}{h_f}\ ,\ \frac{d+d'}{h_f}\ .$$

The dependent variables ((ii) above) are not so easy to obtain. About half a mile of output was obtained from the oscilloscript. Firstly the routine calibrations of the measuring equipment were analysed. A hysterysis effect existed in the measuring equipment which caused slightly different readings to be obtained for the same probe position depending on whether the position was approached by increasing or decreasing probe submergence. Each probe was raised and lowered in still water through several constant increments to heights or depths greater than the anticipated wave heights The resulting trace from the oscilloscript was as shown in Figure AII.1.

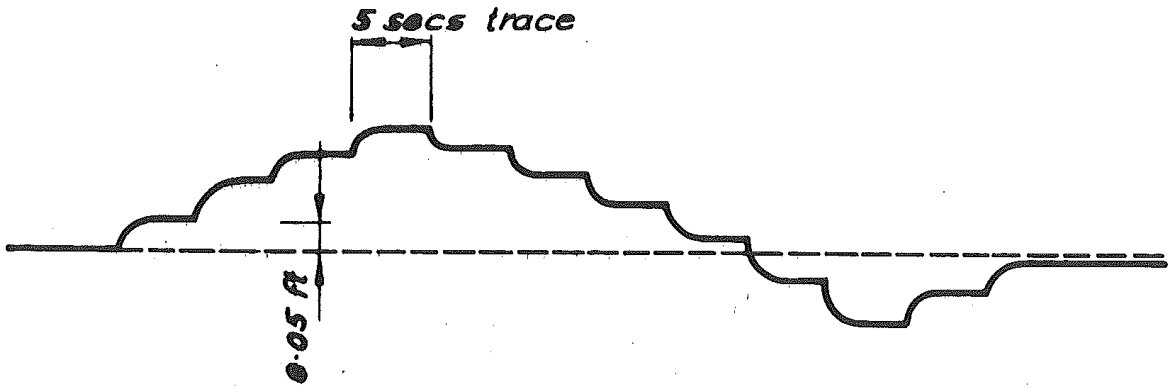

Figure AII.1

Typical Calibration Trace

The simplest method to analyse these calibrations was found to be a graphical one. Graphs of the oscilloscript trace scale versus time during the day were drawn for various probe heights. They were of the form shown in Figure AII.2.

Separate graphs were drawn for increasing and decreasing probe submergence.

Once these calibration curves had been drawn, the wave traces from the oscilloscript could be analysed. For each trace the height of the first four crests and first four troughs were recorded, along with the highest wave in the dispersive wave train. An arbitrary time zero was chosen for each run and the time relative to this zero for each recorded crest and trough to pass each measuring station was noted.

Because each run was repeated once, averages of all readings could be taken to reduce errors. The height readings were divided by the water depth to form parameters $\frac{a}{h_f}$ and $\frac{a'}{h_f}$. Since a time dimension is not thought to be necessary for the description of first wave properties, the time histories of the waves as recorded by the oscilloscript trace were converted into distance histories. A graphical method was found to be most convenient (see Fig. AII.3).

Fig. AII.3 shows how the quantities $\frac{\lambda}{h_f}$ and $\frac{a'}{h_f}$ can be estimated for the instant when the peak of the first wave passes a given point along the channel.

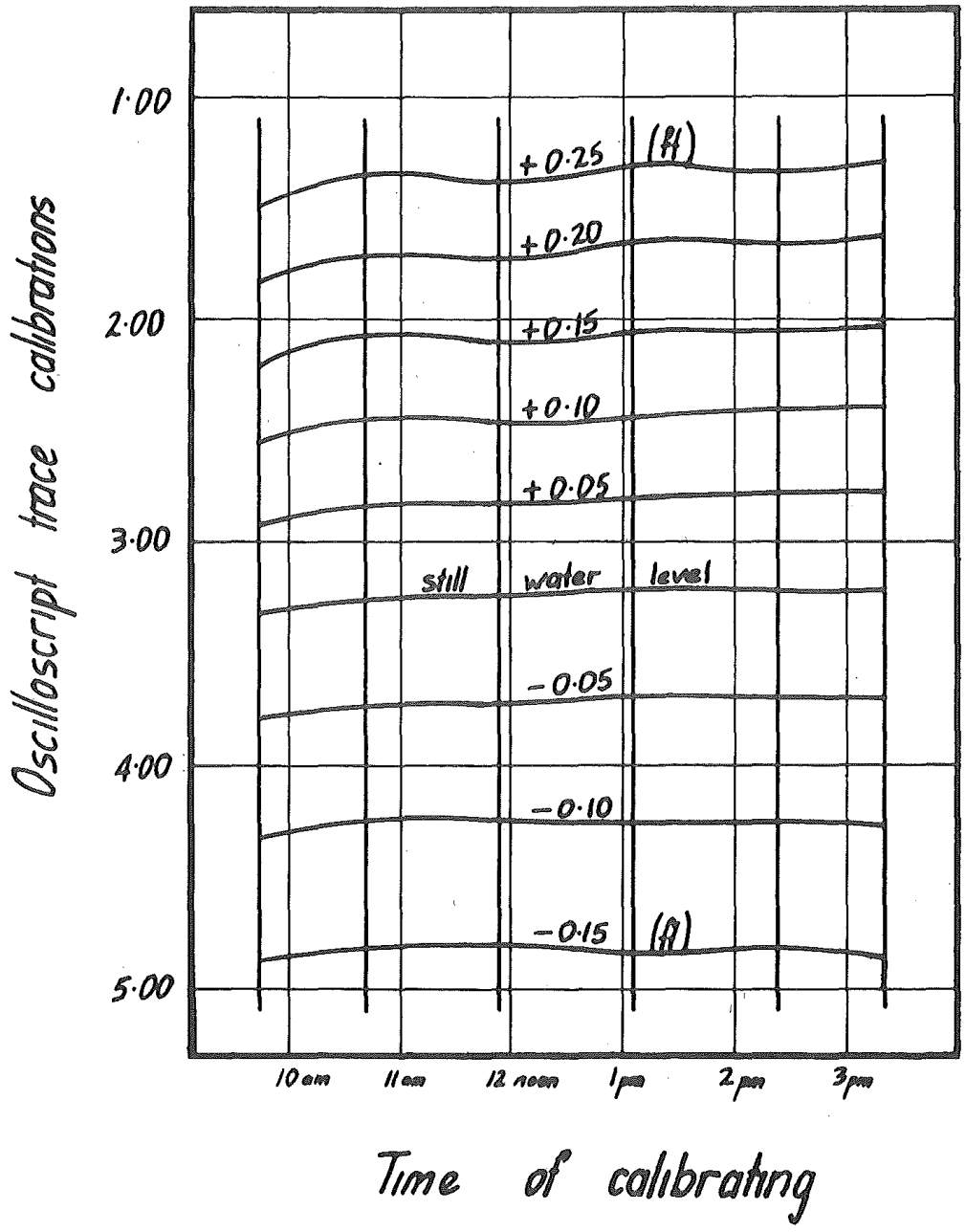

Fig AII.2. Graphical Method of Analysing Calibrations

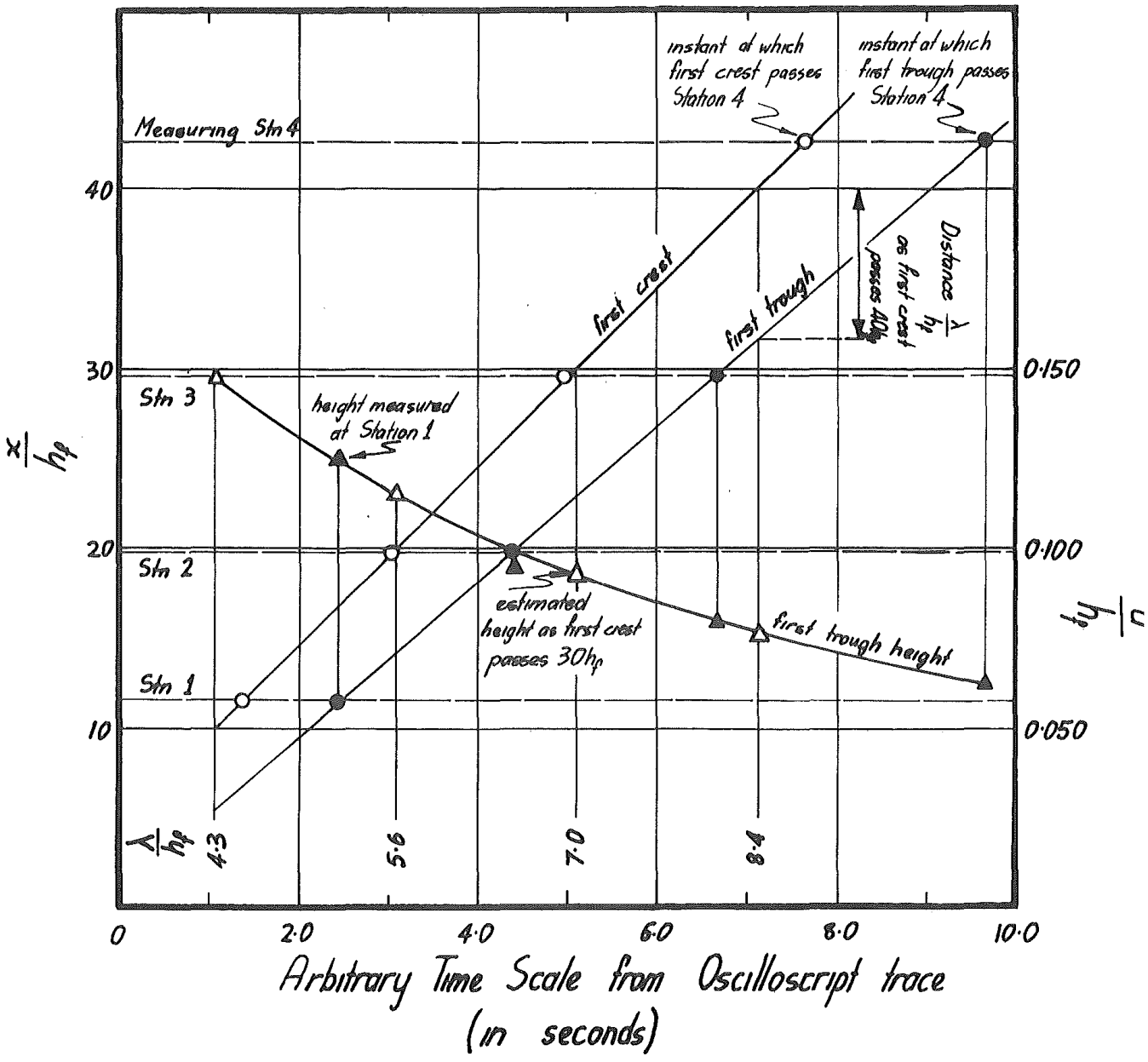

Fig. AII.3. Graphical conversion of time history to distance history.

APPENDIX III

TABULATION OF TEST CONDITIONS

Run	$\frac{H+d'}{h_f}$	$\frac{d'}{h_f}$	$\frac{d+d'}{h_f}$	$\frac{\delta}{h_f}$	$\frac{l}{h_f}$	$\frac{\rho_s d}{\rho_f h_f}$
1	2.04	0.16	0.71	0.07	0.52	1.09
2	1.01	0.19	0.74			
3	1.57	0.17	0.72			
4	2.81	0.23	0.98	0.11	0.71	1.49
5	1.43	0.29	1.04			
6	1.64	0.30	1.11	0.12	0.76	1.61
7	3.03	0.24	1.05			
8	1.14	0.10	0.48	0.08	0.87	0.82
9	1.35	0.11	0.49			
10	1.64	0.11	0.49			
11	1.96	0.11	0.49			
12	1.10	0.13	0.58	0.10	1.03	0.97
13	1.48					
14	1.81					
15	2.22					
16	2.59					

Run	$\frac{H+d'}{h_f}$	$\frac{d'}{h_f}$	$\frac{d+d'}{h_f}$	$\frac{\delta}{h_f}$	$\frac{l}{h_f}$	$\frac{\rho_s d}{\rho_f h_f}$
17	1.10					
18	1.55					
19	2.00	0.16	0.72	0.11	1.28	1.21
20	2.43					
21	1.16	0.20	0.87			
22	1.66	0.20	0.87			
23	2.24	0.19	0.86	0.13	1.53	1.45
24	2.73	0.19	0.86			
25	3.30	0.18	0.85			
26	1.30	0.24	0.97			
27	2.43	0.20	0.93	0.14	1.67	1.57
28	3.59	0.19	0.92			
29	1.36	0.23	1.02			
30	2.63	0.21	1.00			
31	3.20	0.20	0.99	0.15	1.81	1.70
32	1.94	0.22	1.01			
33	3.88	0.19	0.98			
34	2.90	0.18	0.67			
35	2.26	0.18	0.67			
36	1.48	0.19	0.68	0.14	1.13	0.71
37	1.09	0.19	0.68			

Run	$\frac{H+d'}{h_f}$	$\frac{d'}{h_f}$	$\frac{d+d'}{h_f}$	$\frac{\delta}{h_f}$	$\frac{l}{h_f}$	$\frac{\rho_s d}{\rho_f h_f}$
38	1.86	0.06	0.55	0.14	1.13	1.82
39	1.05	0.06	0.55			
40	1.18	0.11	0.84	0.17	1.65	2.65
41	1.55	0.11	0.84			
42	1.90	0.11	0.84			
43	2.38	0.10	0.83			
44	2.37	0.13	0.86	0.17	1.65	2.20
45	1.92	0.14	0.87			
46	1.57	0.15	0.88			
47	1.19	0.15	0.88			
48	1.66	0.28	0.79	0.10	1.16	1.01
49	1.66	0.10	0.61			
50	1.64	0.04	0.55			
51	1.67	0.43	0.94			
52	1.09	0.46	0.97			
53	1.32	0.45	0.96			
54	2.16	0.41	0.92			
55	2.76	0.41	0.92			

Run	$\frac{H+d'}{h_f}$	$\frac{d'}{h_f}$	$\frac{d+d'}{h_f}$	$\frac{\delta}{h_f}$	$\frac{l}{h_f}$	$\frac{\rho_s d}{\rho_f h_f}$
56	2.76	0.34	0.85	Very large	1.17	1.02
57	2.17	0.36	0.87			
58	1.67	0.39	0.90			
59	1.10	0.37	0.88			
60	1.67	0.49	1.00			
61	1.66	0.24	0.75			
62	1.33	0.05	0.56			
63	1.33	0.11	0.62			
64	1.92	0.10	0.61			
65	2.50	0.09	0.60			
66	1.33	0.13	0.64	0.20	1.17	1.02
67	1.34	0.44	0.95			
68	1.34	0.44	0.95	0.32	1.17	1.02
69	1.34	0.12	0.63			
70	1.35	0.43	0.94	0.47	1.17	1.02
71	1.94	0.40	0.91			
72	1.10	0.43	0.94			
73	1.34	0.12	0.63			
74	1.09	0.12	0.63			
75	2.19	0.12	0.63			

Run	$\frac{H+d'}{h_f}$	$\frac{d'}{h_f}$	$\frac{d+d'}{h_f}$	$\frac{\delta}{h_f}$	$\frac{l}{h_f}$	$\frac{\rho_s d}{\rho_f h_f}$
76	2.17	0.10	0.61	0.78	0.59	1.10
77	1.09	0.13	0.64			
78	1.33	0.12	0.63			
79	1.35	0.45	0.97			
80	1.94	0.41	0.93			
81	1.10	0.47	0.99			
82	1.35	0.45	0.97	0.49	0.59	1.10
83	1.34	0.12	0.64			
84	1.34	0.12	0.64	Very Large	0.59	1.10
85	1.34	0.13	0.65	0.22	0.59	1.10
86	1.35	0.47	0.99			
87	1.35	0.29	0.81			

MEASURED FIRST WAVE HEIGHTS

Run	Distance from Block				Water Depth
	16 ft.	27 ft.	40 ft.	58 ft.	(ft)
1	0.143	0.133	0.120	0.106	1.93
2	0.087	0.075	0.068	0.060	1.93
3	0.125		not recorded		1.93
4	0.265	0.230	0.226	0.219	1.42
5	0.159	0.145	0.127	0.120	1.42
6	0.181		not recorded		1.29
7	0.300		" "		1.29
8	0.141	0.121	0.113	0.094	1.81
9	0.163	0.141	0.124	0.119	1.81
10	0.187	0.160	0.143	0.135	1.81
11	0.203	0.179	0.163	0.154	1.81
12	0.179	0.149	0.130	0.117	1.54
13	0.227	0.182	0.175	0.162	1.54
14	0.266	0.218	0.201	0.195	1.54
15	0.295	0.243	0.227	0.220	1.54
16	0.324	0.279	0.253	0.246	1.54
17	0.215	0.211	0.186	0.178	1.21
18	0.292	0.268	0.243	0.235	1.21
19	0.340	0.320	0.304	0.292	1.21
20	0.405	0.364	0.340	0.340	1.21
21	0.291	0.272	0.243	0.248	1.03
22	0.364	0.340	0.325	0.306	1.03
23	0.432	0.422	0.408	0.403	1.03
24	0.510	0.480	0.471	0.466	1.03
25	0.592	0.548	0.534	0.500	1.03
26	0.317	0.296	0.286	0.286	0.95
27	0.518	0.486	0.492	0.486	0.95
28*	0.598	0.518	0.534	0.518	0.95

* broken surge formed

Run	16 ft	27 ft	40 ft	58 ft	Water Depth (ft)
29	0.354	0.337	0.325	0.308	0.88
30*	0.605	0.549	0.560	0.515	0.88
31*	0.560	0.503	0.549	0.503	0.88
32	0.509	0.463	0.463	0.446	0.88
33*	0.560	0.480	0.526	0.480	0.88
34	0.281	0.253	0.235	0.228	1.40
35	0.232	0.218	0.200	0.193	1.40
36	0.193	0.171	0.143	0.146	1.40
37	0.164	0.157	0.128	0.121	1.40
38	0.430	0.399	0.392	0.385	1.40
39	0.252	0.235	0.210	0.214	1.40
40	0.438	0.412	0.400	0.402	0.96
41	0.590	0.559	0.548	0.537	0.96
42		broken surge formed			0.96
43		"	"	"	0.96
44		broken surge formed			0.96
45		"	"	"	0.96
46	0.511	0.475	0.464	0.464	0.96
47	0.391	0.365	0.354	0.344	0.96
48	0.250	0.213	-	0.191	1.36
49	0.286	0.253	-	0.231	1.36
50	0.301	0.250	0.235	0.235	1.36
51	0.209	0.184	0.165	0.158	1.36
52	0.151	0.136	0.125	0.121	1.36
53	0.183	0.158	0.147	0.140	1.36
54	0.242	0.213	0.198	0.198	1.36
55	0.294	0.257	0.250	0.246	1.36
56	0.191	0.177	0.154	0.147	1.36
57	0.158	0.140	0.121	0.118	1.36
58	0.125	0.110	0.099	0.099	1.36
59	0.092	0.077	0.068	0.063	1.36
60	0.096	0.083	0.075	0.072	1.36
61	0.147	0.132	0.118	0.110	1.36
62	0.147	0.130	0.118	0.107	1.36
63	0.131	0.120	0.108	0.097	1.36
64	0.184	0.169	0.156	0.152	1.36
65	0.237	0.219	0.197	0.193	1.36

* broken surge formed

Run	16 ft	27 ft	40 ft	58 ft	Water Depth (ft)
66	0.213	0.195	0.182	0.171	1.36
67	0.169	0.150	0.145	0.132	1.36
68	0.153	0.139	0.126	0.119	1.35
69	0.194	0.176	0.167	0.155	1.35
70	0.146	0.128	0.119	0.111	1.35
71	0.183	0.161	0.148	0.142	1.35
72	0.126	0.109	0.100	0.100	1.35
73	0.183	0.167	0.150	0.144	1.35
74	0.152	0.135	0.126	0.124	1.35
75	0.248	0.230	0.220	0.220	1.35
76	0.117	0.102	0.091	0.087	1.35
77	0.067	0.059	0.056	0.052	1.35
78	0.083	0.076	0.064	-	1.35
79	0.067	0.060	0.054	0.052	1.34
80	0.078	0.065	0.062	0.058	1.34
81	0.062	0.054	0.050	0.048	1.34
82	0.070	0.065	0.054	0.052	1.34
83	0.096	0.080	0.069	0.067	1.34
84	0.060	0.050	0.044	0.041	1.34
85	0.104	0.093	0.082	0.077	1.34
86	0.082	0.073	0.067	0.065	1.34
87	0.095	0.084	0.076	0.071	1.34

Estimated Values of $\frac{a}{h_f}$ for $\frac{H+d'}{h_f} = 100$

Runs	Distance from Block $10h_f$	$20h_f$	$30h_f$	$40h_f$
1- 3	0.082	0.068	0.060	-
4- 5	0.125	0.110	0.100	0.089
6- 7	0.130	-	-	-
8-11	0.130	0.105	0.094	-
12-16	0.174	0.133	0.120	0.113
17-20	0.225	0.193	0.175	0.170
21-25	0.270	0.250	0.228	0.223
26-28	0.275	0.245	0.235	0.230
29-33	0.270	0.260	0.250	0.245
34-37	0.159	0.136	0.125	0.115
38-39	0.245	0.222	0.207	0.198
40-43	0.400	0.358	0.342	0.339
44-47	0.360	0.318	0.300	0.296
51-55	0.150	0.132	0.116	0.115
56-59	0.089	0.071	0.063	0.060
63-65	0.109	0.090	0.082	0.076
70-72	0.123	0.103	0.097	0.092
73-75	0.150	0.130	0.116	0.114
76-78	0.069	0.057	0.053	0.051
79-81	0.062	0.052	0.048	0.047

Measured Values of n at various distances from the block

Runs	Distance from block $10h_f$	$20h_f$	$30h_f$	$40h_f$
1- 3	0.74	0.77	0.84	-
4- 5	0.73	0.76	0.76	0.87
6- 7	0.78	-	-	-
8-11	0.60	0.73	0.69	-
12-16	0.68	0.80	0.77	0.83
17-20	0.74	0.76	0.76	0.76
21-25	0.69	0.75	0.70	0.74
26-28	0.76	0.85	0.83	0.86
29-33	1.03	0.98	1.00	0.95
34-37	0.54	0.59	0.57	0.63
38-39	0.91	1.02	0.95	1.08
40-43	1.03	1.09	1.11	1.08
44-47	0.93	1.03	1.03	0.99
51-55	0.67	0.73	0.70	0.72
56-59	0.79	0.90	0.87	0.87
63-65	0.88	0.97	0.99	1.03
70-72	0.63	0.67	0.72	0.67
73-75	0.67	0.86	0.75	0.82
76-78	0.74	0.74	0.78	0.70
79-81	0.41	0.39	0.36	0.30

Estimated Wave Heights $\frac{a}{h_f}$

Run	Distance from block			
	$10h_f$	$20h_f$	$30h_f$	$40h_f$
1	0.140	0.122	0.105)	Not
2	0.081	0.068	0.060)	recorded
3	0.121		Not recorded	
4	0.268	0.240	0.224	0.216
5	0.162	0.144	0.132	0.121
6	0.188)			
7	0.306)	Not recorded		
8	0.138	0.113	0.103)	
9	0.158	0.130	0.119)	Not
10	0.177	0.147	0.137)	recorded
11	0.197	0.166	0.154)	
12	0.182	0.142	0.127	0.118
13	0.230	0.184	0.169	0.160
14	0.269	0.216	0.200	0.192
15	0.298	0.240	0.222	0.215
16	0.335	0.271	0.251	0.245
17	0.237	0.205	0.190	0.182
18	0.312	0.272	0.251	0.241
19	0.375	0.329	0.307	0.298
20	0.430	0.372	0.346	0.335
21	0.306	0.280	0.262	0.250
22	0.385	0.355	0.338	0.322
23	0.462	0.432	0.420	0.410
24	0.536	0.495	0.480	0.472
25	0.620	0.575	0.550	0.530
26	0.336	0.310	0.295	0.289
27	0.530	0.509	0.496	0.489
28		Broken surge formed		
29	0.370	0.350	0.340	0.328
30		Broken surge formed		
31		" "	"	
32	0.536	0.500	0.475	0.462
33		Broken surge formed		

Run	$10h_f$	$20h_f$	$30h_f$	$40h_f$
34	0.285	0.253	0.235	0.226
35	0.241	0.213	0.199	0.193
36	0.195	0.170	0.154	0.147
37	0.167	0.145	0.132	0.122
38	0.435	0.402	0.390	0.385
39	0.256	0.233	0.217	0.210
40	0.470	0.430	0.410	0.402
41	0.620	0.580	0.560	0.545
42		Broken surge formed		
43		" " "		
44		Broken surge formed		
45		" " "		
46	0.545	0.500	0.475	0.467
47	0.420	0.380	0.360	0.352
48	0.255	0.222	0.203	0.193
49	0.292	0.256	0.235	0.229
50	0.310	0.256	0.239	0.235
51	0.215	0.183	0.167	0.160
52	0.155	0.135	0.125	0.122
53	0.188	0.160	0.147	0.141
54	0.247	0.215	0.199	0.192
55	0.300	0.260	0.245	0.238
56	0.201	0.172	0.156	0.148
57	1.161	0.138	0.124	0.119
58	0.129	0.109	0.102	0.098
59	0.096	0.078	0.068	0.064
60	0.100	0.083	0.075	0.072
61	0.153	0.131	0.118	0.110
62	0.153	0.130	0.117	0.108
63	0.139	0.118	0.107	0.100
64	0.191	0.169	0.157	0.150
65	0.241	0.216	0.200	0.192
66	0.217	0.193	0.181	0.173
67	0.174	0.152	0.141	0.133
68	0.158	0.138	0.127	0.120
69	0.200	0.177	0.165	0.158

Run	$10\,h_f$	$20\,h_f$	$30\,h_f$	$40\,h_f$
70	0.149	0.129	0.119	0.112
71	0.185	0.162	0.150	0.143
72	0.129	0.110	0.102	0.098
73	0.188	0.164	0.151	0.145
74	0.157	0.135	0.126	0.124
75	0.253	0.231	0.222	0.218
76	0.120	0.102	0.092	0.086
77	0.069	0.059	0.055	0.052
78	0.087	0.075	0.068	0.065
79	0.071	0.059	0.054	0.052
80	0.081	0.067	0.061	0.058
81	0.065	0.054	0.050	0.049
82	0.075	0.061	0.055	0.052
83	0.097	0.080	0.071	0.067
84	0.063	0.050	0.044	0.041
85	0.107	0.092	0.083	0.078
86	0.085	0.073	0.067	0.064
87	0.098	0.084	0.076	0.072

Instantaneous values of $\frac{a}{h_f}$, $\frac{a'}{h_f}$, and $\frac{\lambda}{h_f}$ for various runs

Distance from first crest to front of block.

Run	$10\,h_f$			$20\,h_f$		
	$\frac{a}{h_f}$	$\frac{a'}{h_f}$	$\frac{\lambda}{h_f}$	$\frac{a}{h_f}$	$\frac{a'}{h_f}$	$\frac{\lambda}{h_f}$
8	0.138	0.121	3.7	0.113	0.099	5.5
9	0.158	0.136	4.0	0.130	0.109	5.9
10	0.177	0.157	4.0	0.147	0.127	6.0
11	0.197	0.181	4.1	0.166	0.136	6.3
12	0.182	0.120	4.2	0.142	0.100	5.8
13	0.230	0.156	4.4	0.184	0.128	6.4
14	0.269	0.201	4.9	0.216	0.148	6.6
15	0.298	0.194	5.2	0.240	0.158	7.1
16	0.335	0.194	5.4	0.271	0.160	7.4
17	0.237	0.116	4.5	0.205	0.096	6.0
18	0.312	0.151	5.0	0.272	0.122	6.8
19	0.375	0.176	5.2	0.329	0.143	7.4
20	0.430	0.169	5.6	0.372	0.149	8.0
21	0.306	0.102	3.0	0.280	0.086	5.5
22	0.385	0.127	3.5	0.355	0.108	6.0
23	0.462	0.155	4.1	0.432	0.134	7.1
24	0.536	0.155	5.3	0.495	0.134	8.4
25	0.620	0.183	4.0	0.575	0.159	7.5
48	0.255	0.150	4.6	0.222	0.116	6.0
49	0.292	0.180	4.9	0.256	0.142	7.0
50	0.310	0.176	5.0	0.256	0.145	7.1
51	0.215	0.137	4.0	0.183	0.111	5.5
52	0.155	0.087	3.6	0.135	0.067	4.9
53	0.188	0.102	4.2	0.160	0.083	5.5
54	0.247	0.170	5.0	0.215	0.132	6.5
55	0.300	0.177	4.9	0.260	0.144	7.0
56	0.201	-	4.3	0.172	-	6.1
57	0.161	0.148	4.3	0.138	0.115	5.6
58	0.129	0.083	4.3	0.109	0.065	5.5
59	0.096	0.086	4.2	0.078	0.065	5.0
60	0.100	0.102	4.1	0.083	0.077	5.1
61	0.153	0.138	4.3	0.131	0.110	5.0

Run	$30\,h_f$			$40\,h_f$		
	$\frac{a}{h_f}$	$\frac{a'}{h_f}$	$\frac{\lambda}{h_f}$	$\frac{a}{h_f}$	$\frac{a'}{h_f}$	$\frac{\lambda}{h_f}$
8	0.103	0.083	6.7	-	-	-
9	0.119	0.092	7.3	-	-	-
10	0.137	0.103	7.6	-	-	-
11	0.154	0.110	8.0	-	-	-
12	0.127	0.084	7.0	0.118	0.074	8.7
13	0.169	0.105	7.9	0.160	0.089	9.5
14	0.200	0.119	8.4	0.192	0.103	10.6
15	0.222	0.132	9.0	0.215	0.114	11.3
16	0.251	0.134	9.5	0.245	0.114	11.8
17	0.190	0.081	7.6	0.182	0.070	9.0
18	0.251	0.101	8.4	0.241	0.088	10.3
19	0.307	0.118	9.6	0.298	0.100	11.7
20	0.346	0.132	10.4	0.335	0.118	12.7
21	0.262	0.072	7.3	0.250	0.062	9.0
22	0.338	0.095	8.5	0.322	0.086	10.6
23	0.420	0.116	10.0	0.410	0.104	13.0
24	0.480	0.120	12.0	0.472	0.110	15.0
25	0.550	0.144	12.1	0.530	0.131	16.4
48	0.203	0.096	7.7	0.193	0.086	9.5
49	0.235	0.113	8.6	0.229	0.094	10.5
50	0.239	0.121	8.8	0.235	0.104	10.7
51	0.167	0.091	7.0	0.160	0.074	8.5
52	0.125	0.053	6.1	0.122	0.043	7.3
53	0.147	0.068	6.7	0.141	0.056	7.9
54	0.199	0.105	8.0	0.192	0.088	9.6
55	0.245	0.117	8.9	0.238	0.098	10.9
56	0.156	-	7.8	0.148	-	9.5
57	0.124	0.093	7.0	0.119	0.077	8.4.
58	0.102	0.053	6.6	0.098	0.047	7.8
59	0.068	0.052	5.9	0.064	0.045	6.8
60	0.075	0.061	6.1	0.072	0.052	7.1
61	0.118	0.090	5.8	0.110	0.075	6.6

Quantities $f(\frac{\delta}{h_f}, \frac{d'}{h_f})$ and $\frac{\frac{a}{h_f}}{\frac{1}{h_f} \cdot f(\frac{\delta}{h_f}, \frac{d'}{h_f})}$ * as used in Figures 7.12, 7.13.

Run	$f(\frac{\delta}{h_f}, \frac{d'}{h_f})$	Distance from block $10h_f$	$20h_f$	$30h_f$	$40h_f$
1- 3	0.84	0.188	0.156	0.137	-
4- 5	0.75	0.236	0.208	0.189	0.168
6- 7	0.73	0.234	-	-	-
8-11	0.85	0.176	0.142	0.127	-
12-16	0.83	0.205	0.157	0.141	0.133
17-20	0.80	0.220	0.189	0.171	0.166
21-25	0.77	0.230	0.212	0.194	0.189
26-28	0.75	0.220	0.196	0.188	0.184
29-33	0.75	0.200	0.193	0.185	0.182
34-37	0.77	0.183	0.156	0.144	0.132
38-39	0.83	0.262	0.238	0.222	0.212
40-43	0.78	0.310	0.278	0.265	0.263
44-47	0.77	0.285	0.252	0.237	0.234
51-55	0.62	0.210	0.185	0.163	0.161
56-59	0.72	0.213	0.170	0.151	0.144
63-65	0.94	0.200	0.165	0.150	0.139
70-72	0.49	0.214	0.179	0.169	0.160
73-75	0.62	0.209	0.181	0.161	0.159
76-78	0.57	0.207	0.171	0.156	0.153
79-81	0.45	0.234	0.196	0.181	0.177

* This quantity assumes that although $\frac{\delta}{h_f}$ and $\frac{d'}{h_f}$ were always finite (except for $\frac{\delta}{h_f}$ in runs 56-65) the value of $\frac{a}{h_f}$ for $\frac{\delta}{h_f}$ and $\frac{d'}{h_f}$ equal to zero can be obtained by dividing $\frac{a}{h_f}$ by $f(\frac{\delta}{h_f}, \frac{d'}{h_f})$. Division of $\frac{a}{h_f}$ by $\frac{1}{h_f}$ gives the equivalent value of $\frac{a}{h_f}$ for $\frac{1}{h_f} = 1.00$.

Velocities of first crests and troughs at $30\,h_f$ from the block. (In most cases the velocities were ostensibly constant over the range $x = 10\,h_f$ to $40\,h_f$. An asterick (*) marks those cases where the velocity increased slightly over the first $20\,h_f$ or more)

Run	$\frac{V}{(gh_f)^{\frac{1}{2}}}$	$\frac{V'}{(gh_f)^{\frac{1}{2}}}$
8	1.02*	0.95*
9	1.07*	0.90*
10	1.11*	0.85*
11	1.07*	0.88*
12	1.03	0.90
13	1.05	0.88
14	1.07	0.88
15	1.07	0.88
16	1.09	0.88
17	1.06	0.92
18	1.09	0.90
19	1.13	0.88
20	1.13	0.86
21	1.09	0.93*
22	1.14*	0.91*
23	1.20*	0.88*
24	1.22*	0.96*
25	1.24*	0.88*
48	1.05	0.88*
49	1.05	0.88
50	1.07	0.89
51	1.05	0.89
52	1.03	0.88
53	1.03	0.90
54	1.05	0.90
55	1.09	0.88
56	1.03	0.86
57	1.03	0.88
58	1.03	0.90
59	0.99	0.90*
60	0.99	0.90
61	0.99	0.90*

BIBLIOGRAPHY

1. J.E. Prins, "Characteristics of waves generated by a local disturbance", Trans. American Geographical Union, Vol. 39, No.5, Oct. 1958, pp. 865-874.

2. L. Law and A. Brebner, "On Water Waves Generated by Landslides", Proc. Third Australasian Conf. on Hydraulics and Fluid Mechanics, 1968, pp. 155-159.

3. R.L. Weigel, "Laboratory studies of gravity waves generated by the movement of a submerged body", Trans. American Geographical Union, Vol. 36, Oct. 1955, No.5, pp. 759-774.

4. R.L. Weigel, E.K. Noda, E.M. Kuba, D.M. See and G.F. Tornberg, "Water Waves Generated by Landslides in Reservoirs", Journal of the Waterways and Harbors Division, Proc. American Society of Civil Engineers, Vol. 96, No. WW2, May 1970, pp. 307-333.

5. E. Buckingham, "Model Experiments and the Form of Empirical Equations", Trans. American Society of Mechanical Engineers, Vol. 37, 1915, pp. 263-296.

6. G.H. Keulegan, "Gradual Damping of Solitary Waves", Journal of Research of the National Bureau of Standards, Vol.40, Research Paper RP1895, June 1948, pp. 487-498.

7. D.J. Miller, "Giant Waves in Lituya Bay, Alaska", U.S. Geologcial Survey Professional Paper 354-C, 1960.